Pathways to global hydrogen production within planetary boundaries

Supplementary materials

Michaël Lejeune[1,2], Sami Kara[1,2*], Michael Zwicky Hauschild[4,5*], Sareh Shahrabifarahani[1], Rahman Daiyan[2,3*]

[1] Sustainability in Manufacturing and Life Cycle Engineering Research Group, School of Mechanical and Manufacturing Engineering, The University of New South Wales, Sydney 2052, Australia.

[2]Australian Research Council, Training Centre for the Global Hydrogen Economy, Sydney 2052, Australia.

[3]School of Minerals and Energy Engineering, The University of New South Wales, Sydney 2052, Australia.

[4]Division for Quantitative Sustainability Assessment (QSA), Department of Environmental and Resource Engineering, Technical University of Denmark, Kgs, Lyngby, Denmark.

[5]Centre for Absolute Sustainability, Technical University of Denmark, Kgs, Lyngby, Denmark.

Table of Contents

Introduction

This document provides supporting information for the main script. When possible, underlying data and raw figures are included in the Zenodo repository: https://doi.org/10.5281/zenodo.14416523. Additionally, this document contains various acronyms to enhance readability. Therefore, we have summarised the key acronyms in Table 1.

Table 1. **Definition of essential acronyms**.

Acronym	Description
PBI	Planetary boundaries interaction
N-PBI	Planetary boundaries interaction scenario: no interactions
B-PBI	Planetary boundaries interaction scenario: Biophysically mediated interactions
H-PBI	Planetary boundaries interaction scenario: Full range of interactions (reactive human-mediated, biophysically mediated interactions and parallel impacts)
IPCC AR6	Intergovernmental Panel for Climate Change, 6th assessment report
IAM	Integrated assessment model
SSP	Shared-socioeconomic pathway
SSPx	x stands for the family of SSP (e.g., 1,2,5)
REMIND	REgional Model of INvestments and Development
PkBugd500	500GtCO_2 emission budget from 2020 to 2100
SOS	Safe operating space
aSOS	Allocated safe operating space
EI	Energy imbalance (change in radiative forcing)
[CO_2]	Change CO_2 concentration
OA	Ocean acidification
AAL	Atmospheric aerosol loading
FWU	Freshwater use
PBF	Phosphorus biochemical flow
NBF	Nitrogen biochemical flow
SOD	Stratospheric ozone depletion
LSC	Land system change
BI	Biosphere integrity

Environmental space allocation for large-scale hydrogen production

This section details the analysis to define the environmental space allocation for global hydrogen production. First, a brief review of the allocation principles and factors used in the literature is presented. This is followed by a comprehensive data analysis based on the IPCC AR6[1,2], which is presented and explained. Then, the rationale behind the modelling choice of the environmental space allocation factor is discussed, and finally, the global safe operating space is established.

A brief review

Absolute environmental sustainability assessment (AESA) studies mainly follow Bjørn et al.[3] recommendations. This review focuses on the allocation principles that can define an environmental space for an anthropogenic system. These allocation principles are usually based on distributive justice theory[3,3–5] and many combinations may be used depending on the goal and scope of the study. Bjørn et al.[3] recommended using a multitude of allocation principles to quantify potential uncertainties related to the definition of the environmental space for an anthropogenic system. Indeed, the allocation principle is the most sensitive and uncertain parameter in AESA studies. However, the most commonly used allocation principles in the literature remain grandfathering-based[4,5].

Grandfathering-based principles rely on the status quo, meaning that today's anthropogenic systems are assigned space proportionately to their current emission intensities or economic performance[3–6]. However, using current emission intensities or economic performance is far from ideal because the allocation principle would not align with the planetary boundaries, which require a change of human operations. As explained in the main script, the environmental space allocation should be linked to a scenario leading to human operations within the safe operating space to be meaningful towards the planetary boundaries. For instance, Heide et al.[7] show the difference between a static and dynamic environmental space allocation and how the allocated space is intimately linked to a climate target (i.e., 1.5°C vs 2°C). Yet, to our knowledge, no ASEA studies focusing on global hydrogen production have implemented this crucial aspect comprehensively.

Only a few studies have carried out an AESA of the production of hydrogen and its derivates[8–11]. Weidner et al.[8] focused on hydrogen production pathways and allocated a large environmental space for global hydrogen production equivalent to ~10% of the global SOS. First, by using an energy emission-based grandfathering allocation factor (73.2%) based on today's (2023) values to create an initial environmental space and then downscaled the allocated space further using the final energy demand for hydrogen in 2050 (13.5% based on a 2.6W/m^2 radiative forcing climate target). In comparison, Salah et al.[9], who also focused on hydrogen production pathways, found 0.07% by applying an economic-based utilitarian principle. In addition, D'Angelo et al. focused on low-carbon ammonia production routes, and recently, D'Angelo et al. focused on the valorisation of flue gas for synthetic natural gas and ammonia production. In both studies, hydrogen is used as a feedstock. These studies, however, do not specify the allocation factor value. In all studies, the functional unit is treated as temporally constant, which is deemed unrealistic by Guinée et al.[12]. Also, the climate context is not considered by Salah et al.[9] and is partially addressed by Weidner et al.[8], where a mix of grandfathering and future-oriented allocation factors based on a 2°C scenario is used.

As explained in the main script, only IAM-based scenarios limiting global warming to 1.5°C (or 1.9W/m² by 2100) would be meaningful for a planetary boundaries-based assessment. Indeed, it is the only scenario that ensures mitigation towards planetary boundaries for climate change[13]. Also, shared socio-economic pathway (SSP) scenarios inherently tackle the social aspect as they maximise socio-economic welfare at regional levels to meet their respective climate targets[14]. Consequently, we based our analysis on a collection of SSP scenarios from various IAM models in the IPCC AR6[1,2] database. We focus on scenarios leading to 1.9W/m² radiative forcing by 2100.

Data collection and analysis

The integrated assessment models used in the space allocation were taken from the IPCC AR6[1,2] except for the REMIND-PkBugd500 models sourced from premise[15]. A model preselection was conducted to include models that satisfied an effective radiative forcing nearing 1.9±0.2 W/m² (based on the 50th percentile) by 2100 (see Figure 1). Further models were excluded based on their depth of assessment. For instance, models that did not include – (i) comprehensive hydrogen pathway, (ii) gross CO_2 emissions at a global and secondary energy level or elements to derive these variables. Some models have a 10-year time resolution. Linear interpolation was conducted to increase the time resolution to a 1-year step for the cumulative sums. The complete list of IAMs selected for the environmental space allocation is summarised in Table 3.

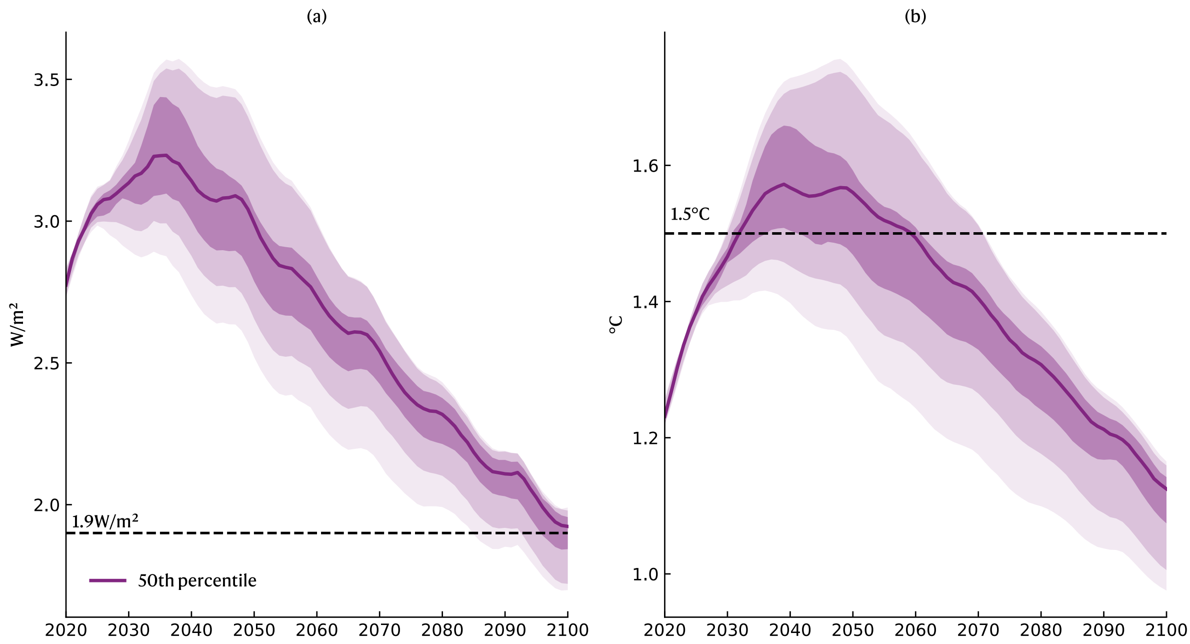

Figure 1. **Climate target results derived from collecting IAM scenarios from the IPCC AR6[1,2]** (sample size n=20). (a) evolution of the radiative forcing. (b) Evolution of the temperature anomaly with slight overshoot (IPCC AR6 category C1[2]). The solid purple line refers to median values. From the median values outwards, different shades of purples are structured as follows: 25th -75th, 5th -95th interquartile ranges and min-max.

Figure 2 shows the calculated cumulative emissions, annual hydrogen production rates and the dynamic allocation principle ratio. As can be interpreted from Figure 2.a, the median trajectory of the selected scenarios nears with a slight overshoot, the 500GtCO_2 cumulative emissions targets from 2020 to 2050 defined by the IPCC AR6[16] to limit global warming to 1.5°C with >50% confidence. In comparison, all REMIND SSPx-PkgBudg500 are strictly in line with their nameplate target and consistent with the 90% confidence interval from the derived trajectory.

We further quantified the role of hydrogen in the reference scenario and compared it against all REMIND SSPx-PkgBudg500 and the IEA NZE[17] projections (Figure 2.b). One notable difference between the PkgBudg500 SSP1 and 5 is the adaptation and climate mitigation challenges. SSP1 has low climate mitigation and adaptation challenges, leading to reduced annual hydrogen production. We found that the annual production rate for hydrogen in the SSP1-PkgBudg500 is the most consistent with the reference model ~300MtH_2/yr by 2050. In contrast, SSP5-PkgBudg500 has high climate mitigation and low adaptation challenges. Due to its decarbonisation potential, the scenario requires significantly more electrolytic hydrogen production ~1200MtH_2/yr by 2050. As can also be seen, the SSP5 scenario represents the maximum annual hydrogen production. Because it is well beyond the confidence intervals of the selected scenarios and it is deemed rather unrealistic. On the other hand, SSP2 has a medium challenge in terms of adaptation and climate change mitigation. It is found to be more in line with IEA projections[18] and within the 90% confidence interval. In this scenario, by 2050, the annual hydrogen production will reach 490 MtH_2/yr.

Table 2. **List of integrated assessment models for a 1.5°C by 2100 climate target used for environmental space allocation.** The * symbol indicates models available in the premise Python software to update the background database but not in the IPCC AR6 dataset[1]. The † symbol indicates the reference model used in this work. The ° symbol indicates an unknown version of an IAM model. The REMIND-PkBugd500 models are not part of the IPCC AR6 data[1] but were added to the stack of climate-viable models based on their reported climate temperature range.

Model	Scenario
REMIND 2.1	CEMICS_HotellingConst_1p5
REMIND ° -MAgPIE 2.1	PkBugd500 – SSP1*†
	PkBugd500 – SSP2*
	PkBugd500 – SSP5*
REMIND 1.7	CEMICS-1.5-CDR20
	ADVANCE_2030_1.5C-2100
	CEMICS-1.5-CDR12
	ADVANCE_2020_1.5C-2100
REMIND-MAgPIE 1.7-3.0	PEP_1p5C_red_eff
	CD-LINKS_NPi2020_400
	SMP_1p5C_Def
	SMP_1p5C_regul
	PEP_1p5C_full_NDC
	PEP_1p5C_full_goodpractice
	SMP_1p5C_Sust
	PEP_1p5C_full_eff
	CD-LINKS_INDC2030i_400
	SMP_1p5C_lifesty
POLES ADVANCE	ADVANCE_2030_1.5C-2100
	ADVANCE_2020_1.5C-2100

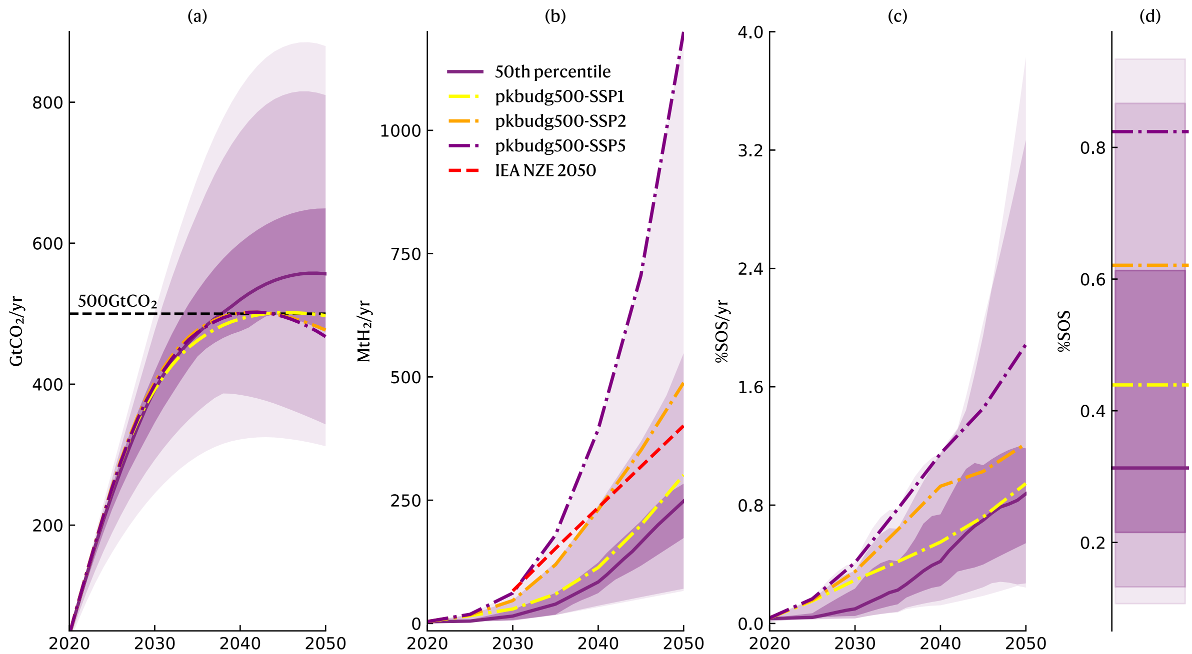

Figure 2. **Prospective environmental budget/space for global hydrogen production.** (a): Cumulated global CO_2 emissions from the selected models compared against the REMIND SSPx-PkgBudg500 scenarios and the 500GtCO_2 target from the IPCC AR6[16]. (b): Global annual hydrogen production rate trends from selected models compared against the REMIND SSPx-PkgBudg500 scenarios and projections from IEA[18]. (c): Dynamic allocation principle ratio using the selected models compared against all REMIND SSPx-PkgBudg500 scenarios. (d): Static allocation principle ratio for the period (2020-2050) using the selected models compared against all REMIND SSPx-PkgBudg500 scenarios. The solid purple line in this figure refers to median values (sample size n=20). From the median values outwards, different shades of purples are structured as follows: 25^{th} -75^{th}, 5^{th} -95^{th} interquartile ranges, and the minimum and maximum values.

Figure 2.c represents the calculated allocation principle ratio for the annual hydrogen supply. In comparison to previous work, the environmental space is dynamic. For instance, from nearly 0% in 2020, it gradually increases to ~0.9% (median values) by 2050. When the dynamic results over the period of this work and the allocation principle ratio are averaged, it is found to be 0.33%/year based on the median value. As can also be seen from Figure 2.c, all SSPx-PkgBudg500 are at least within the 90% confidence interval, with SSP1-PkgBudg500 being the closest from the median trajectory. Similarly, static values were observed for the allocation principle of 0.44%/year, 0.62%/year, and 0.82%/year for SSP1, 2 and 5, respectively (see Figure 2.d).

Overall, we find the SSP1-PkgBudg500 to be the closest model matching SSP to the general trajectory for global hydrogen production. For this reason, the main script focuses on this SSP.

Environmental space allocation

In the main script, the environmental space allocation factor is defined as in Equation 1. The principle behind this factor was defined in such a way that it would capture the declining emissions of the energy industry and the growing contribution of hydrogen supply in the energy sector.

$$\alpha_{H_2} = \frac{E_{gross,SE}}{E_{gross}} \times \frac{SE_{H_2}}{SE} \quad (1)$$

To this extent, as explained in the main script, emission-based allocation to downscale the safe operating space to the global energy supply was used. The utilitarian principle defined in this work is a combination of the calorific content (CC) and production volume (PO). Bjørn et al.[3] initially defined the CC principle for food, but in theory, it could equally be applied to chemicals using heating values. From a unit perspective, both represent specific units of energy typically expressed as energy (J) per unit of mass or volume. Second, the PO principle is also applicable to this work. It is, however, a broad term that can account for the scaling of a production unit. Building on this and knowing that SSP scenario results are typically expressed in EJ/yr, the CC and PO principles would be involved. Using the total secondary energy SE to normalise SE_{H_2} would naturally consider the energy content of hydrogen compared to other secondary energy sources but also account for the scale of hydrogen. The complete list of allocation principles reviewed, including comments on the acceptance or rejection of each principle, is provided in Table 3.

We note that a specific gross CO_2 emission factor is available for hydrogen in the SSPx-PkgBudg500 scenario outputs. However, this was not implemented because using an emission-based allocation principle only would not capture the growing utility of hydrogen in these scenarios. For instance, using equation 2, the allocation factor would unreasonably expect the hydrogen production to be near emission-free between 2040 and 2050 (see Figure 3a). Given the mismatch between the SSP scenario and prospective LCA results[19,20], significant transgression levels would be observed for these years. For this reason, Equation 1 is found to be more appropriate (see Figure 3b).

Lastly, the allocation of the global safe operating space (SOS) was done using the data from Table 4.

$$\alpha_{H_2} = \frac{E_{gross,SE_{H_2}}}{E_{gross}} \quad (2)$$

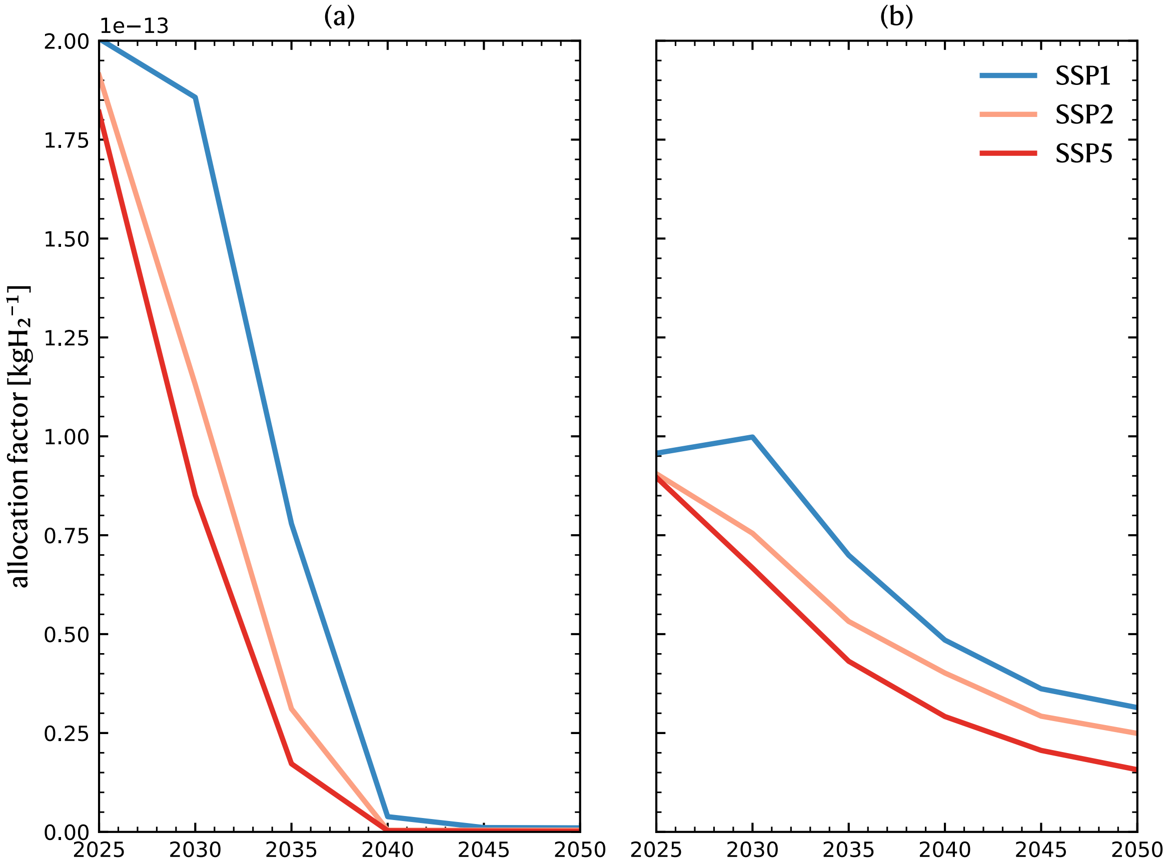

Figure 3. **Comparison of environmental allocation factors.** (a) Emission-based allocation factor using Equation 2. (b) Emission-utilitarian-based allocation factor using Equation 1. Results are normalised with the total hydrogen production derived from each SSP scenario. Note: data used for this representation only SSPx-PkBudg500 scenarios.

Table 3. **List of allocation principles reviewed** based on refs[3–5].

Ethical norm	Allocation principle	Acronym	Inclusion or rejection	Source
Egalitarian	Equal per capita	EPC	Rejection: The scope of the study is global, hence for the entire population.	[3]
Inegalitarian	Grandfathering	GF	Rejection: Integrated assessment model scenarios are used in this work. Projections into the future are available, and there is no need for a reference year to allocate based on the status quo.	[3]
	Land area	LA	Rejection: Non-global	[3]
Utilitarian	Economic added value	EVA	Rejection: No data is available for the future trajectory of hydrogen in the 1.5°C scenario.	[3]
	Final consumption expenditure	FCE	Rejection: No data is available for the future trajectory of hydrogen in the 1.5°C scenario.	[3]
	Cost efficiency	CE	Rejection: No data is available for the future trajectory of hydrogen in the 1.5°C scenario.	[3]
	Calorific content	CC	Included: The secondary energy supply of hydrogen accounts for the energy content.	[3]
	Physical production output	PO	Included: The secondary energy supply of hydrogen accounts for the scale.	[3]
Prioritarian	Historical debt	HD	Rejection: Non-global	[3]
	Capability to reduce	CR	Rejection: Non-global	[3]
	Ability to pay	AtP	Rejection: Non-global	[5]
Sufficientarian Egalitarian & Utilitarian	Fulfilment of Human Needs	FHN	Rejection: Non-global and no data available for the future trajectory of hydrogen in the 1.5°C scenario.	[4]

Table 4. **Global safe operating space definition for each biophysical system**. Data used originates from refs[21,22].

Biophysical system	Planetary boundary X_{PB}	Natural background X_0	Safe operating space	Unit
Climate change-Energy imbalance	1	0	1	W/m^2
Climate change-CO2 Concentration	350	278	72	ppm
Ocean acidification-Carbonate ion concentration	2.752	3.44	0.688	Ωarag
Atmospheric aerosol loading-Aerosol Optical Depth (AOD)	0.14	0.25	0.11	Aerosol optical depth
Freshwater use-Global	4000	0	4000	km^3
Biogeochemical flows-P	26.2	20	10	TgP
Biogeochemical flows-N	62	0	62	TgN
Stratospheric ozone depletion-Stratospheric O3 concentration	275	290	15.0	Dobson units
Land-system change-Global	75	100	25	%
Biosphere Integrity-Change in biosphere integrity	90	100	10	%

Life cycle inventories

This section details the life cycle inventories used for the bottom-up system modelling carried out in this work. All inventories were updated using the premise[15] python software and based on each year of the SSPx-PkgBudg500 scenarios.

To provide a wide range of options to the technology choice model, twelve hydrogen production pathways were considered and summarised in Table 5. These sources include all key hydrogen production pathways coined to play a key role in the future hydrogen economy, such as electrolytic-, biomass- or fossil-based hydrogen production pathways[23,24]. These technologies are coupled with a carbon removal and sequestration option when applicable.

Similarly, we provide a broad range of options for sources of electricity, including conversions between the different voltage classes. The conversions were done assuming a conversion efficiency of 95% and modifying the "electricity voltage transformation from high to medium voltage | DE" and "electricity voltage transformation from medium to low voltage | DE" inventories to allow choices between electricity sources. The considered inventories are summarised in Table 6.

Lastly, the sensitivity analysis assumes a concurrent direct air capture of carbon dioxide process. For this, we selected two processes, one relying on a steam input for its operation and the other on heat from a heat pump. These inventories are summarised in Table 7.

Table 5. **List of hydrogen production pathway inventories for global hydrogen production.** Inventories were obtained from the premise software[15] and modified to reflect each year of the SSPx-PkgBudg500 scenarios. The ecoinvent v3.9.1 "cut-off by classification" was used to this extent. CH= Switzerland.

Acronym	Reference flow: Hydrogen, gaseous	Location	Source
AEC	hydrogen production, gaseous, 20 bar, from AEC electrolysis, from choice electricity	World	[25]
BIOccs	hydrogen production, gaseous, 25 bar, from gasification of woody biomass in entrained flow gasifier, with CCS, at gasification plant	World	[26]
bioSMR	hydrogen production, steam methane reforming, from biomethane	World	[26]
bioSMRccs	hydrogen production, steam methane reforming, from biomethane, with CCS	World	[26]
CG	hydrogen production, coal gasification	World	[27]
CGcss	hydrogen production, coal gasification, with CCS	World	[26]
MP	hydrogen production, gaseous, 100 bar, from methane pyrolysis	World	[28]
PEM	hydrogen production, gaseous, 30 bar, from PEM electrolysis, from choice electricity	World	[25]
SMR	hydrogen production, steam methane reforming	World	[26]
SMRccs	hydrogen production, steam methane reforming, with CCS	World	[26]
SOECsteam	hydrogen production, gaseous, 1 bar, from SOEC electrolysis, from choice electricity	World	[25]
SOECelectricity	hydrogen production, gaseous, 1 bar, from SOEC electrolysis, from choice electricity and steam	CH	[29]

Table 6. **List of inventories for the electricity requirement of global hydrogen production.** Inventories were obtained from the premise software[15] and modified to reflect each year of the SSPx-PkgBudg500 scenarios. The ecoinvent v3.9.1 “cut-off by classification” was used to this extent. RoW=rest of the world.

Acronym	Reference flow: 1kWh of electricity at, [a]high voltage, [b]medium voltage, [c]low voltage	Location	Source
Biomass$_{IGCC}$	electricity production, at biomass-fired IGCC power plant[a]	World	[15,30]
Coal	electricity production, hard coal[a]	RoW	[15,30]
Coal$_{c}$	electricity production, hard coal, subcritical[a]	RoW	[15,30]
Coal$_{ccs}$	electricity production, at hard coal-fired power plant, post, pipeline 200km, storage 1000m[a]	RoW	[31]
Coal$_{IGCC}$	electricity production, at hard coal-fired IGCC power plant[a]	World	[15,30]
Coal$_{oxy,fired}$	electricity production, at hard coal-fired power plant, ultra-super critical, oxy, pipeline 200km, storage 1000m[a]	GLO	[31]
Coal$_{uc}$	electricity production, hard coal, ultra-supercritical[a]	World	[15,30]
Fossil	electricity production, medium voltage, petroleum refinery operation[b]	RoW	[15,30]
Geothermal	electricity production, deep geothermal[a]	World	[15,30]
Hydro	electricity production, hydro, run-of-river[a]	RoW	[15,30]
Hydrogen	electricity production, from hydrogen-fired one gigawatt gas turbine[a]	World	[15,30]
Lignite	electricity production, lignite[a]	World	[15,30]
Lignite$_{ccs}$	electricity production, at lignite-fired power plant, post, pipeline 200km, storage 1000m[a]	World	[31]
Lignite$_{IGCC}$	electricity production, at lignite-fired IGCC power plant[a]	World	[15,30]
NG	electricity production, natural gas, gas turbine, conventional power plant[a]	RoW	[15,30]
NG$_{ccs}$	electricity production, at natural gas-fired combined cycle power plant, post, pipeline 200km, storage 1000m[a]	World	[31]
NG$_{steam}$	electricity production, natural gas, subcritical, steam cycle[a]	RoW	[15,30]
Nuclear$_{bwr}$	electricity production, nuclear, boiling water reactor[a]	RoW	[15,30]
Nuclear$_{phwr}$	electricity production, nuclear, pressure water reactor, heavy water moderated[a]	World	[15,30]
Nuclear$_{pwr}$	electricity production, nuclear, pressure water reactor[a]	RoW	[15,30]
oil	electricity production, oil[a]	RoW	[15,30]

Peat	electricity production, peat[a]	World	[15,30]
SolarCSP	electricity production, solar tower power plant, 20 MW[a]	RoW	[15,30]
Solar$_{CSP,p}$	electricity production, solar thermal parabolic trough, 50 MW[a]	RoW	[15,30]
SolarPV	electricity production, photovoltaic, 570kWp open ground installation, multi-Si[c]	RoW	[15,30]
Wind	electricity production, wind, >3MW turbine, onshore[a]	RoW	[15,30]

Table 7. **List of inventories for the direct capture and storage of atmospheric carbon dioxide**. Inventories were obtained from the premise software[15] and modified to reflect each year of the SSPx-PkgBudg500 scenarios. The ecoinvent v3.9.1 "cut-off by classification" was used to this extent.

Acronym	Reference flow: 1kgCO_2 captured and stored	Location	Source
DAC$_{steam}$	Carbon dioxide, captured from atmosphere and stored, with a solvent-based direct air capture system, 1MtCO2, with industrial steam heat, and choice electricity	World	[32]
DAC$_{HP}$	carbon dioxide, captured from atmosphere and stored, with a solvent-based direct air capture system, 1MtCO2, with heat pump heat, and choice electricity	World	[32]

Planetary boundary interaction model

The planetary boundaries interaction (PBI) model used in this work follows that of Lade et al.[33]. The framework relies on control theory where feedback loops lead to an amplification or mitigation of impact on a control variable $\boldsymbol{x}$ (see Figure 4).

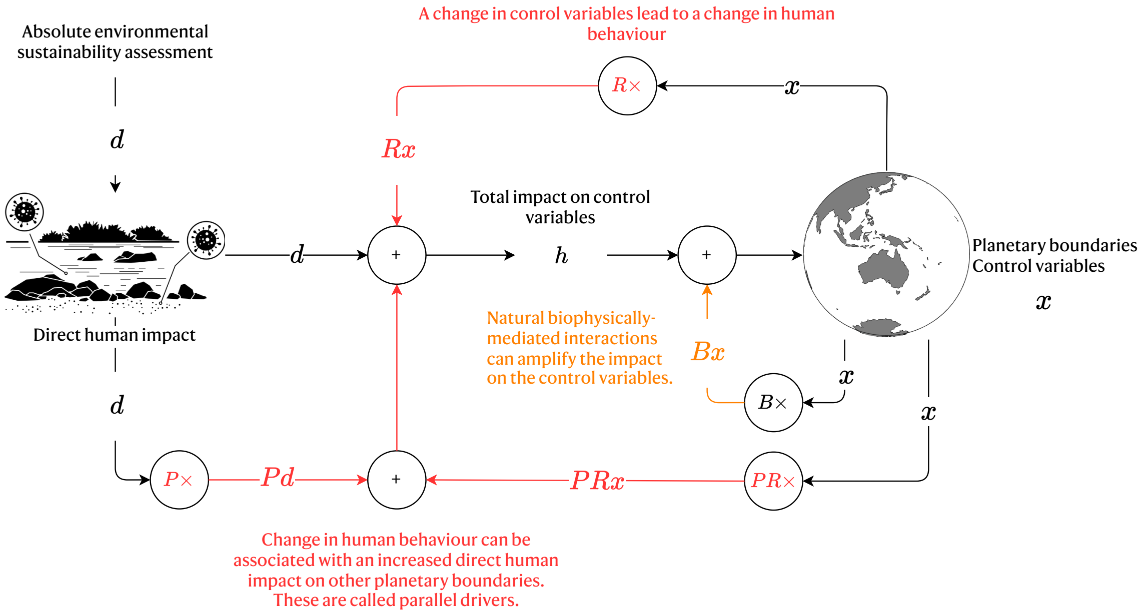

Figure 4. **Control theory framework used in this work.** Adapted from Lade et al.[33].

In this work, we extend the framework by incorporating the normalised direct human impact $\boldsymbol{d}$ as a result of the planetary boundary-based prospective life cycle assessment (see equation 3). In this equation, $\boldsymbol{\Gamma}$ is the interaction matrix built using the control theory framework from Lade et al.[33]. As mentioned in the main script. It is possible to limit the interactions to biophysically mediated interactions (equation 4) or consider the full range of interactions equation (5). Further, $\boldsymbol{I}$ is the identity matrix, $\boldsymbol{B}$ is the matrix of biophysically mediated interactions, $\boldsymbol{R}$ the reactive human-mediated interactions, $\boldsymbol{P}$ is the parallel human driver matrix. The role of these matrices is illustrated in Figure 4. All interactions are extensively detailed in Lade et al.[33] and, therefore, for more details on how data used in this work were defined, we refer the reader to Lade et al.[33]. The computed $\boldsymbol{\Gamma}$ matrices are represented by Figure 5 for the biophysically mediated interactions matrix and Figure 6 for the full range of interactions.

$$\boldsymbol{\Gamma d} = \boldsymbol{x} \tag{3}$$

$$(\mathbf{I} - \mathbf{B})^{-1} = \boldsymbol{\Gamma}_{\mathbf{B}} \tag{4}$$

$$[\boldsymbol{I} - (\boldsymbol{B} + \boldsymbol{R} + \boldsymbol{PR})]^{-1}(\boldsymbol{I} + \boldsymbol{P}) = \boldsymbol{\Gamma}_{\mathbf{H}} \tag{5}$$

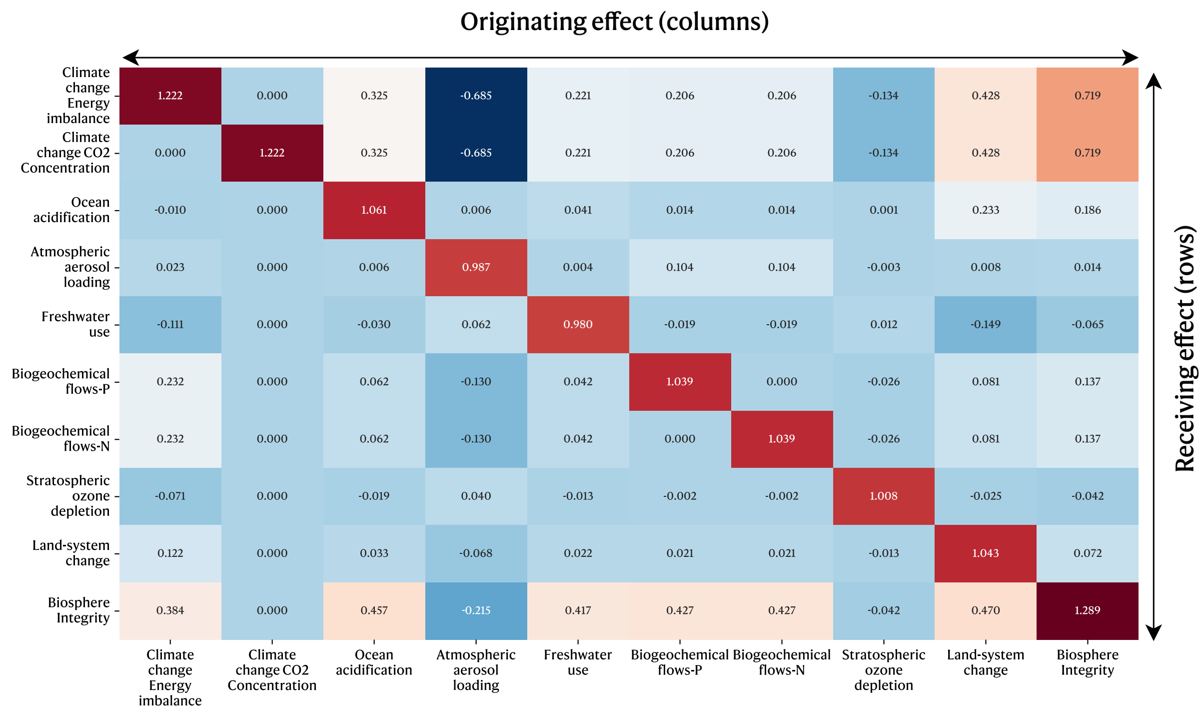

Figure 5. **Biophysical interactions matrix Γ from equation 5.** Note that the underlying data originates from Lade et al.[33].

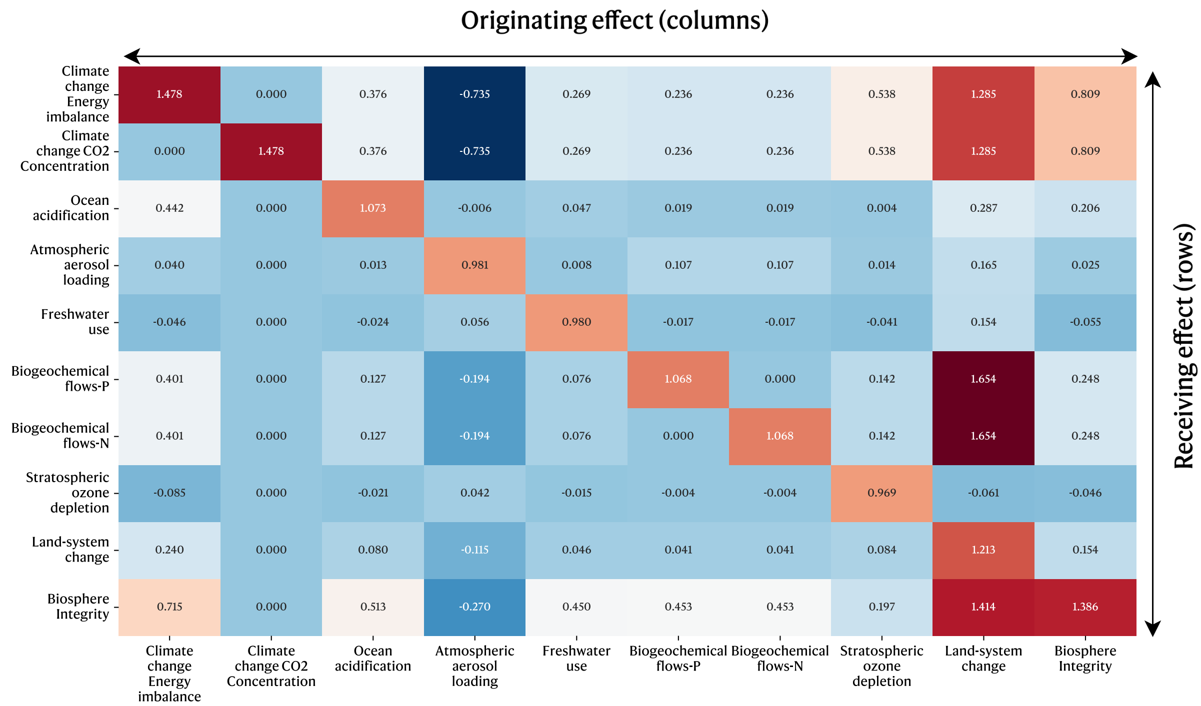

Figure 6. **Interaction matrix for the full range of interactions Γ derived from equation 6.** Note that the underlying data originates from Lade et al.[33].

To adapt the dimensions of the model from Lade et al.[33] to this work had to be made. Notable changes include the disaggregation of the global control variable for climate change into radiative forcing and CO_2 concentration boundaries. A similar process was done to disaggregate biochemical flows into a boundary for the nitrogen and phosphorus flows.

For the climate change control variable, because these control variables are not independent (linked by the radiative efficiency of CO_2), we nullified the influence of the CO_2 concentration control variable on other control variables to avoid doubling the interactions from climate change. This is because we assumed that radiative forcing is a more stringent control variable and, therefore, more appropriate. Note that while the originating effect from the CO_2 concentration is nullified, our model still enables the control variable to receive effects from other control variables.

Regarding the biochemical flows, phosphorus and nitrogen flows are treated as independent control variables with a common driver, i.e., agricultural activities. Because of this, the disaggregation is more straightforward. We applied the same interactions to and from other control variables for phosphorus and nitrogen flows. This assumption is also based on that of Lade et al.[33] where the authors state that these control variables are interchangeable.

While the PBI model is at an infancy stage, it provides a solid base to guide the technology choice model in selecting processes to minimise the impact on the planetary boundaries with consideration of potential interactions. To the best of our knowledge, integrating potential interactions with AESA has never been attempted. Therefore, the approach in this work is novel and significantly contributes to the field of AESA. The matrices used in this work were built using the exact data from Lade et al.[33].

Hydrogen production system model

This section provides further detail on the mathematical formulation used for constraining the energy system model represented in this work (see Figure 7). It is important to note that the present system is resolved for each five-year step of the 2025-2050. Since each five-year step is treated discretely, all calculations omit the temporal variable to improve clarity. The temporal dimension is contained in the integrated assessment model data. The goal of our bottom-up model is to find, for each temporal step, a system that minimises the occupation/transgression of the allocated safe operating space and considers potential interactions between planetary boundaries.

As the SSP does not provide enough resolution on the type of electricity to be supplied to the hydrogen subsystem, one of the objectives of this work is to define, using a bottom-up approach, the electrical mix to ensure a minimum impact on the planetary boundaries. To do so, we define a share of the electricity allocated to hydrogen production using the allocation factor in Equation 6. In this equation, SE stands for secondary energy expressed in EJ/yr. This allocation factor is then used in equation 7 to define the maximum capacity c_e for each energy source e. Also, in this equation, m_{H_2} refers to the total mass of hydrogen and is obtained using equation 8. In this equation, we based our calculation on the lower heating value of hydrogen, i.e., 33.33kWh/kgH_2, to convert the EJ/yr unit to the annual energy rate in kgH_2/yr.

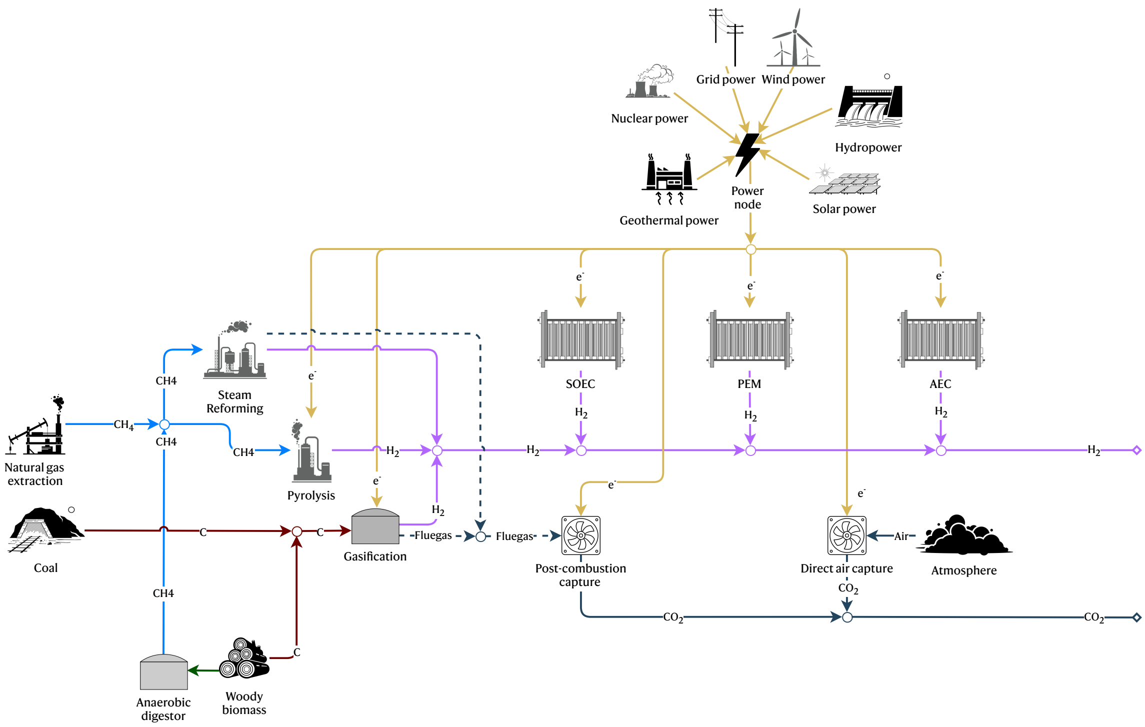

Figure 7. **Simplified representation of the global hydrogen production system.** Dashed lines indicate an optional pathway. PEM= Proton exchange membrane electrolysis. SOEC= Solid oxide electrolysis. AEC= Alkaline electrolysis.

$$\beta = \frac{SE_{H_2}}{SE} \ [-] \tag{6}$$

$$c_e = \frac{SE_e}{3.6 \times 10^{-12}} \beta \, m_{H_2}^{-1} \quad \left[\frac{kWh}{kg_{H_2}}\right] \; \forall e \in E \tag{7}$$

$$m_{H_2} = \frac{SE_{H2}}{3.6 \times 10^{-12} \times 33.33} \quad \left[\frac{kg_{H_2}}{yr}\right] \tag{8}$$

The SSP and LCA results do not match, notably in terms of the electricity requirement required for hydrogen production. Thus, we found necessary to introduce a unitless slack variable ϵ_e when constraining the scale of an energy source s_e (see equation 9). This variable represents an additional share of the capacity c_e and allows the model to go beyond the capacity initially defined by the SSP. To remain realistic, we limited the use of the slack variable ϵ_e to wind and solar PV sources only. That means, for all other sources ϵ_e is set to zero. This is because these sources have a faster deployment rate than other electricity generation sources and are more likely to provide the additional electricity capacity for global hydrogen production. We note also that equation 6 can be formulated differently to decouple ϵ from the capacity. In that case, the inequality constraint becomes $s_e \leq c_e + \epsilon_e$ and would represent an additional capacity in kWh/kgH_2 instead of a factor. If the model remains within the electricity capacity available for wind or solar, ϵ_e will effectively become 0. When the model requires more capacity from wind or solar, gate constrain defined by expression 10 comes into place. When no upper value is specified for ϵ_e , both wind and solar become unconstrained. In contrast to that, when a maximum value $\epsilon_{e,max}$ is defined, the model has a limited degree of freedom to overscale these electricity sources. In such a case, the model will use the next electricity source with the lowest environmental impact. For this case study, our model does not impose a $\epsilon_{e,max}$ and capacity for both wind and solar PV are unconstrained.

$$s_e \leq (1 + \epsilon_e) \, c_e \qquad \forall e \in E \tag{9}$$

$$\begin{cases} 0 \leq \epsilon_e \leq \epsilon_{e,max} \\ 0 \leq \epsilon_e \end{cases} \quad \forall e \in E \tag{10}$$

So far, the model only set maximum constraints for each electricity source. However, many electricity mixes can be defined within the solution space. This can lead to a technology with a relatively large capacity constraint, unrealistically providing most of the electricity. For instance, the capacity for solar energy is large enough such that wind electricity would not be part of the mix as the technology choice model[34] (TCM) will always opt for the electricity source with the lowest environmental impact and in proportion with the available capacity. To avoid this issue, the equality constraint (equation 11) is defined, and the goal is to force wind and solar to be represented in the proportions defined by the SSP scenario. To this extent, we use the factor $\frac{SE_{\text{SolarPV}}}{SE_{\text{Wind}}}$ which represents the ratio of the secondary energy supply of solar photovoltaic electricity over wind electricity.

$$s_{\text{SolarPV}} \frac{SE_{\text{SolarPV}}}{SE_{\text{Wind}}} = s_{\text{Wind}} \tag{11}$$

Regarding the bottom-up model of hydrogen sources, the constraints were defined in two ways. When a maximum capacity for a technology h is known, it is directly (with equation 13) used to constrain the scale s_h of that particular technology. For instance, water electrolysis technologies' maximum capacities were calculated directly from the scenario results of Wei et al.[23]. it is important to note that while this study[23] reports production scales for some of the hydrogen technologies used in this work, we limited their use to hydrogen technologies only. This has the benefit of giving more degrees of freedom to the TCM for the bottom-up modelling of the hydrogen production system. Indeed, the degree of freedom is created with equation 14, where only a maximum capacity for a group of technologies c_{group} is known. For instance, hydrogen production from natural gas could be provided via methane pyrolysis or steam methane reforming. The group containing these technologies would be limited by the total capacity for natural gas-based hydrogen production set by the SSP scenario. This gives the TCM the necessary degrees of freedom to create a mix within a group of technologies.

$$s_h \leq c_h \quad \forall h \in H \tag{13}$$

$$\sum_h s_h = c_{group} \quad \forall h \in H_{group} \in H \tag{14}$$

Table 8 **Description of the mathematical set E**, describing all electricity production technologies and related constraints. The unit of the scaling factors and constraints is kWh/kgH_2, as defined by equation 7. For each group, the constraint is defined by the SSPx-PkBudg500 scenarios. LCI process acronyms are detailed in Table 6. SE=Secondary energy.

Subset	Description	SSP scenario group constrain variable	LCI Process	Technology constraint
E_{wind}	Electricity production from wind	SE|Electricity|+|Wind	Wind	Equation 11
E_{solar}	Electricity production from solar	SE|Electricity|Solar|+|PV	SolarPV	Equation 11
		SE|Electricity|Solar|+|CSP	SolarCSP	Equation 7
			$Solar_{CSP,p}$	Equation 7
E_{coal}	Electricity production from coal	SE|Electricity| Coal |+|w/o CC	Coal	Equation 7
			$Coal_{c}$	Equation 7
			$Coal_{uc}$	Equation 7
			$Coal_{IGCC}$	Equation 7
			$Coal_{oxy,fired}$	Equation 7
$E_{coal,ccs}$	Electricity production from coal with carbon removal	SE|Electricity|Coal|+|w/ CC	$Coal_{ccs}$	Equation 7
E_{hydro}	Electricity production from hydro energy	SE|Electricity|+|Hydro	Hydro	Equation 7
$E_{nuclear}$	Electricity production from nuclear energy	SE|Electricity|+|Nuclear	$Nuclear_{bwr}$	Equation 7
			$Nuclear_{phwr}$	Equation 7
			$Nuclear_{pwr}$	Equation 7
$E_{geothermal}$	Electricity production from geothermal energy	SE|Electricity|+|Geothermal	Geothermal	Equation 7
$E_{biomass}$	Electricity production from biomass	SE|Electricity|+|Biomass	$Biomass_{IGCC}$	Equation 7
$E_{gas,ccs}$	Electricity production from gas with carbon removal	SE|Electricity|Gas|+|w/ CC	NG_{ccs}	Equation 7

E_{gas}	Electricity production from gas	SE|Electricity|Gas|+|w/o CC	NG	Equation 7
			NG_{steam}	
E_{oil}	Electricity production from oil	SE|Electricity|+|Oil|	oil	Equation 7
E_{other}	Electricity production from alternative sources which cannot be classified under the variables of the IAM scenario	Unconstrained	Fossil	Unconstrained
			Hydrogen	
			Lignite	
			$Lignite_{ccs}$	
			$Lignite_{IGCC}$	
			Peat	

Table 9 **Description of the mathematical set H**, describing all hydrogen production technologies. The scaling factor unit and constraints are in $kgH_{2,\ sourced}/kgH_{2,\ supplied}$. For each group, the constraint is defined by the SSPx-PkBudg500 scenarios. LCI Process acronyms are detailed in Table 5. SE=Secondary energy.

Subset	Description	IAM scenario group constrain variable	LCI Process	Technology constraint
$H_{electrolysis}$	Electrolytic hydrogen production processes	SE|Hydrogen|+|Electricity	AE	Wei et al.[23]
			PEM	Wei et al.[23]
			SOECsteam	Wei et al.[23]
			SOECelectricity	Wei et al.[23]
H_{Bio}	Biomass-based hydrogen production	SE|Hydrogen|Biomass|+|w/o CC	bioSMR	Unconstrained
$H_{Bio,ccs}$	Biomass-based hydrogen production with carbon removal	SE|Hydrogen|Biomass|+|w/ CC	bioSMRccs	Unconstrained
			BIOccs	Unconstrained
H_{gas}	Natural gas-based hydrogen production	SE|Hydrogen|Gas|+|w/o CC	MP	Unconstrained
			SMR	Unconstrained
$H_{gas,ccs}$	Natural gas-based hydrogen production with carbon removal	SE|Hydrogen|Gas|+|w/ CC	SMRccs	Unconstrained
H_{coal}	Coal-based hydrogen production	SE|Hydrogen|Coal|+|w/o CC	CG	Unconstrained
$H_{coal,ccs}$	Coal-based hydrogen production with carbon removal	SE|Hydrogen|Coal|+|w/ CC	CGcss	Unconstrained

Extended system results

This section provides more insights into the optimised system. Since the H-PBI scenario shows negligible difference for the system model, it is neglected in this section. First, Figure 8 shows the contribution of each hydrogen production pathway in each of the SSPx-PkBugd500 scenarios. These results are identical to those reported in Figure 3 of the main script but provide a clearer representation of the contribution of technologies. Second, to evaluate the potential production scale of the hydrogen production pathways, we applied equation 16 and represented the results in Figure 9. Lastly, the bottom-up electrical mix to supply the system in each SSPx-PkBugd500 and planetary boundaries interaction scenario is provided in Figure 10.

$$C_k = s_h \frac{SE_{H2}}{3.6 \times 10^{-6} \times 8760 \times C_f} \ [GW] \quad \forall h \in H \tag{16}$$

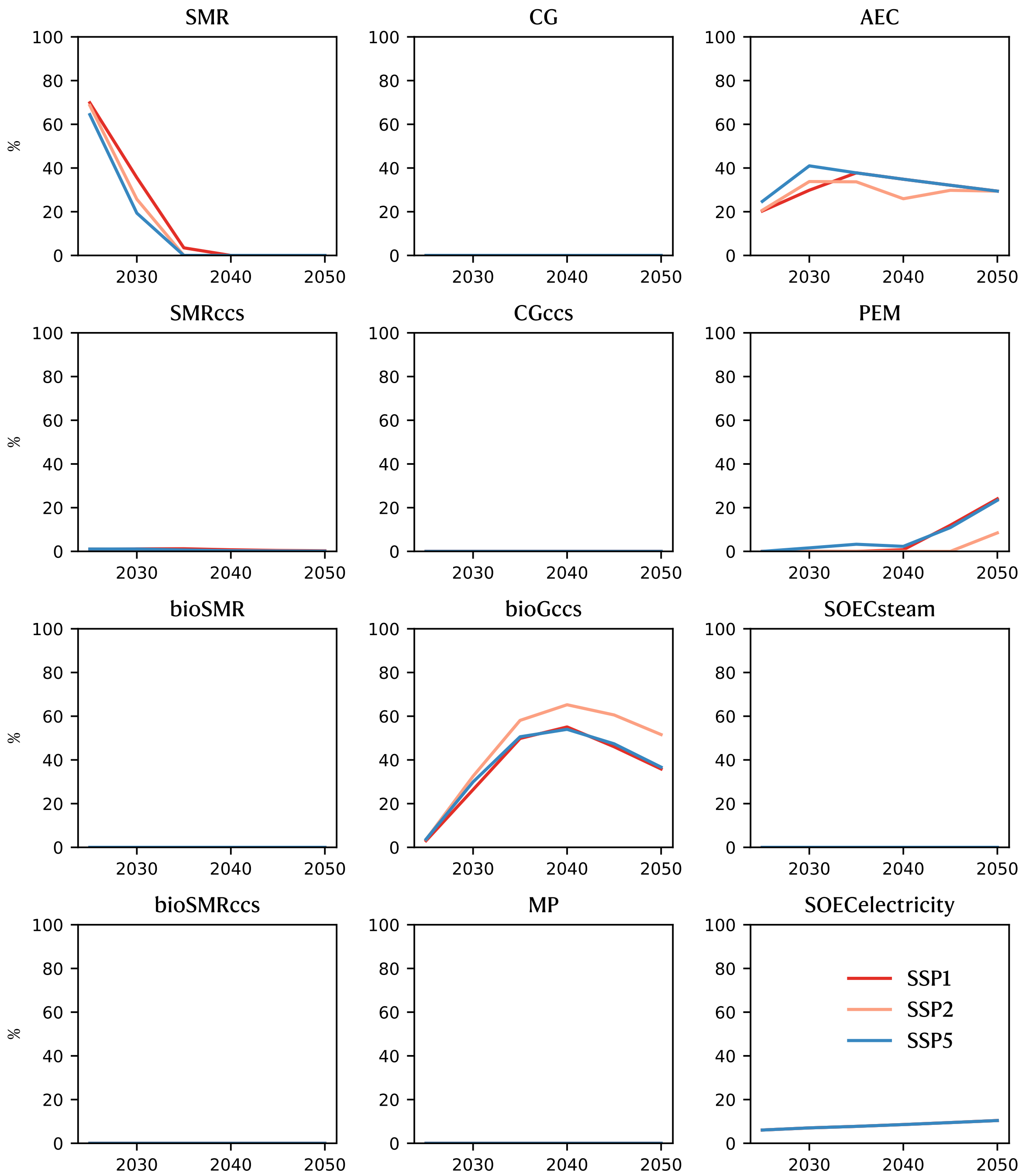

Figure 8. **Share of electrolytic hydrogen production per production pathway and SSPx-PkBugd500 scenario.** Results are based on the B-PBI scenario, which is identical to the N-PBI scenario. Note that these contributions are identical to those reported in Figure 3 of the main script. LCI Process acronyms are detailed in Table 5.

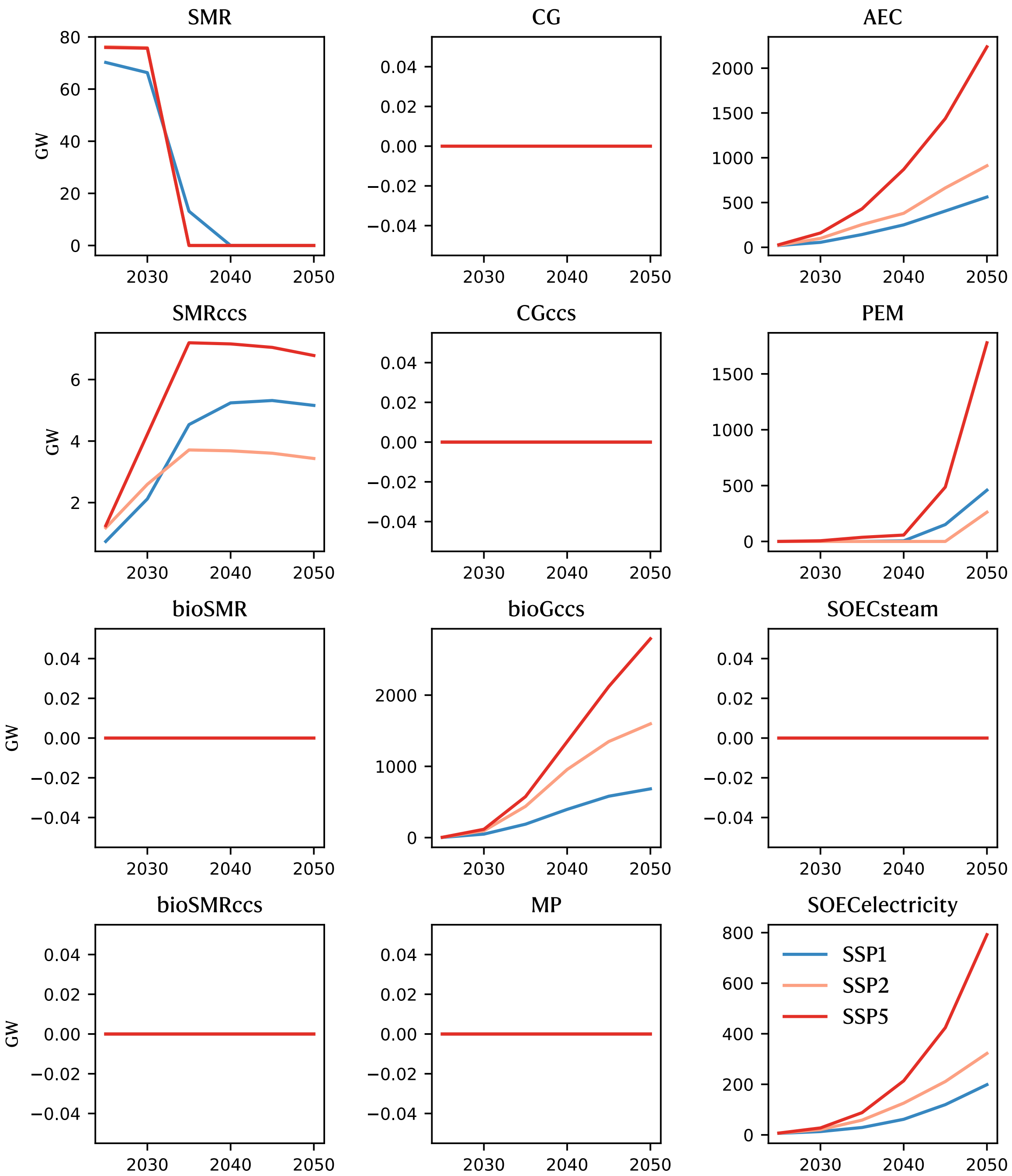

Figure 9. **Computed annual capacities per hydrogen production pathways and SSP for the N-, B-PBI scenarios.** These results are based on an assumed capacity factor of 0.6. LCI Process acronyms are detailed in Table 5.

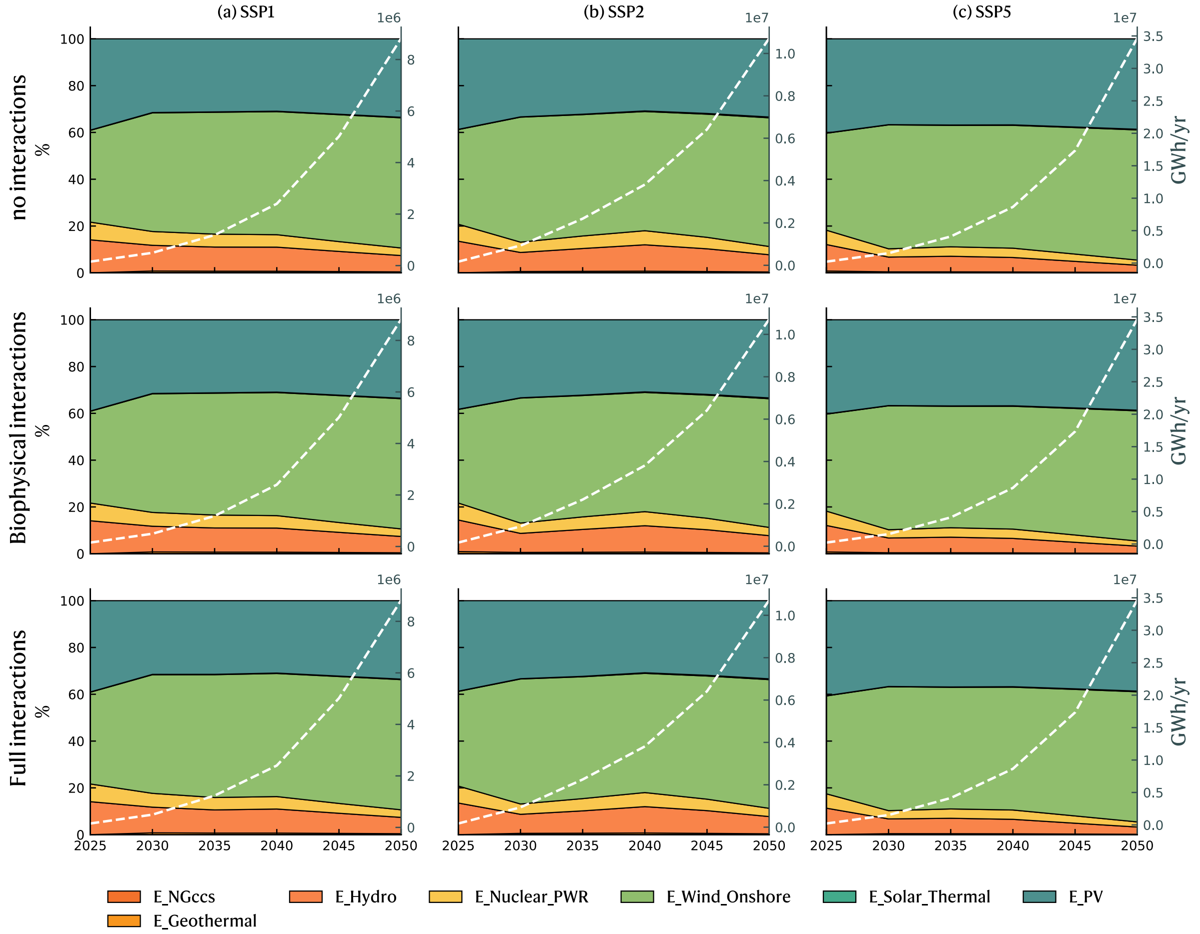

Figure 10. **Electrical mixes.** The white dashed lines represent the total annual energy the system requires (right axis). E = Electricity. Details for the Acronyms can be found in Table 6.

Impact assessment

Contribution analysis

In this section, a collection of figures (11 to 22) describing the key life cycle processes contributing to the overall impact in the N-PBI and B-PBI scenario. Contribution plots for the H-PBI scenario are available in the supplementary data along with the underlying data. The cut-off criterion is set to 5% of the impact. In other words, processes contributing to less than 5% of the overall impact are aggregated into a common "other" category.

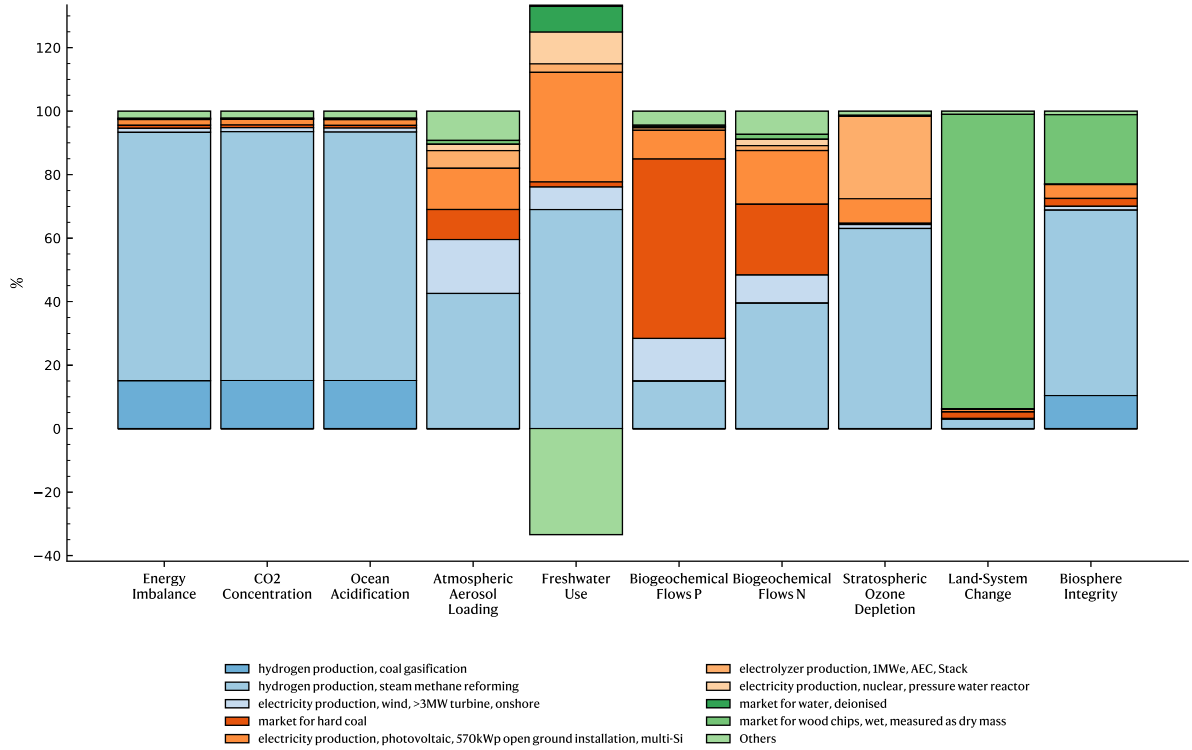

Figure 11. **Contribution analysis for 2025 and SSP1 scenario.**

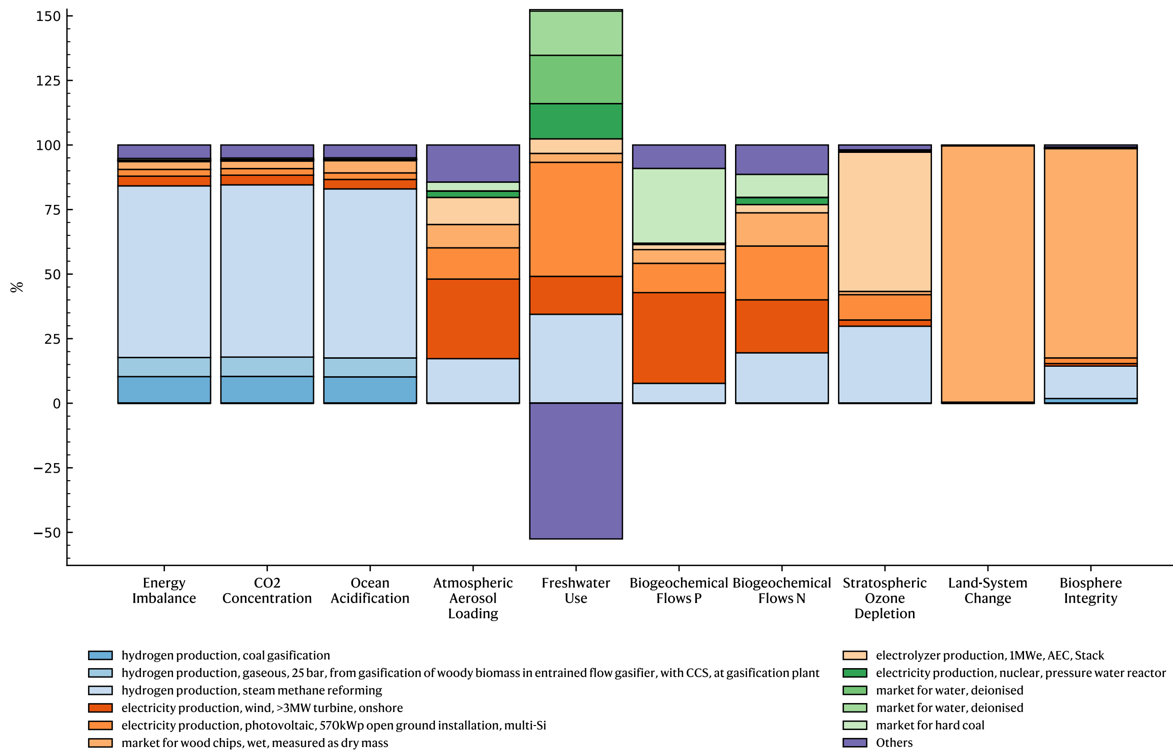

Figure 12. **Contribution analysis for 2030 and SSP1 scenario.**

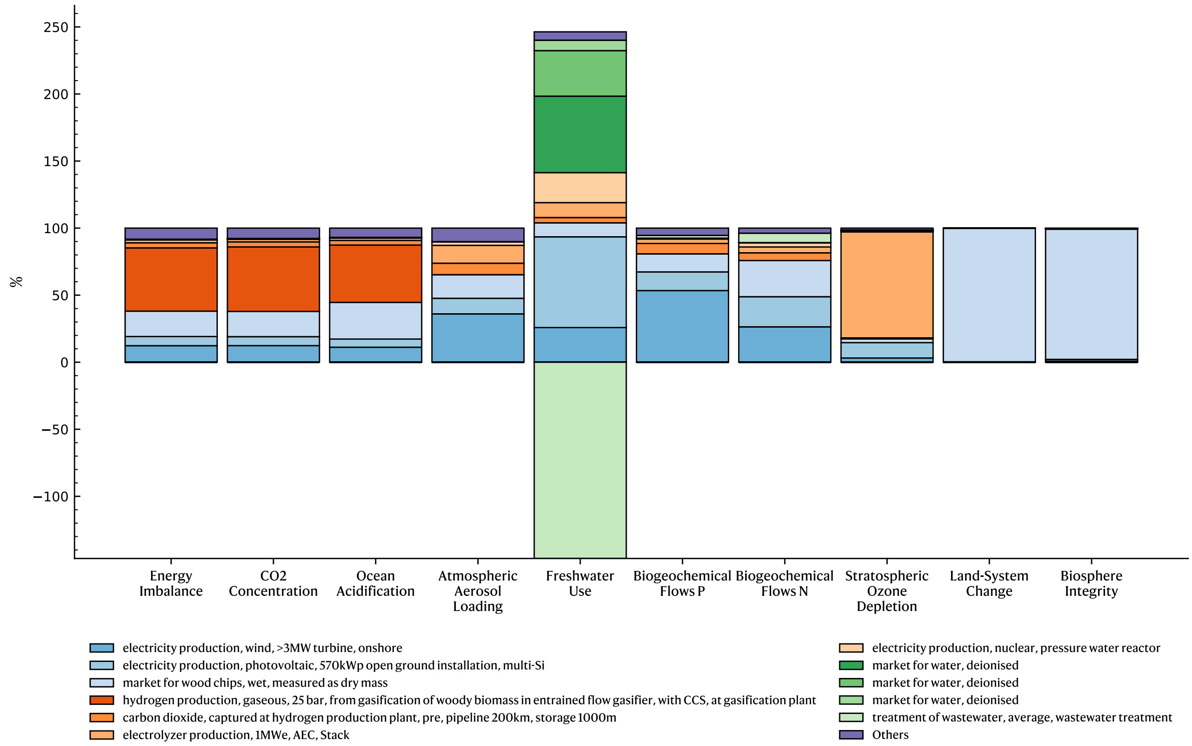

Figure 13. **Contribution analysis for 2040 and SSP1 scenario.**

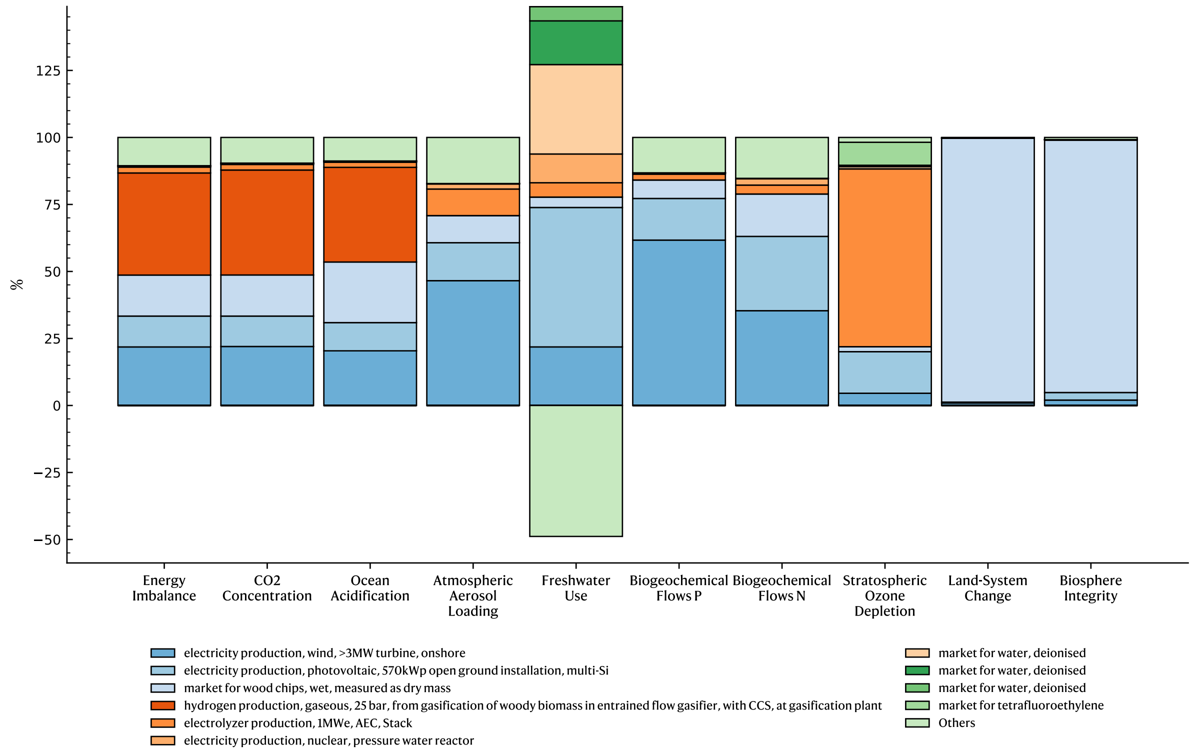

Figure 14. **Contribution analysis for 2050 and SSP1 scenario.**

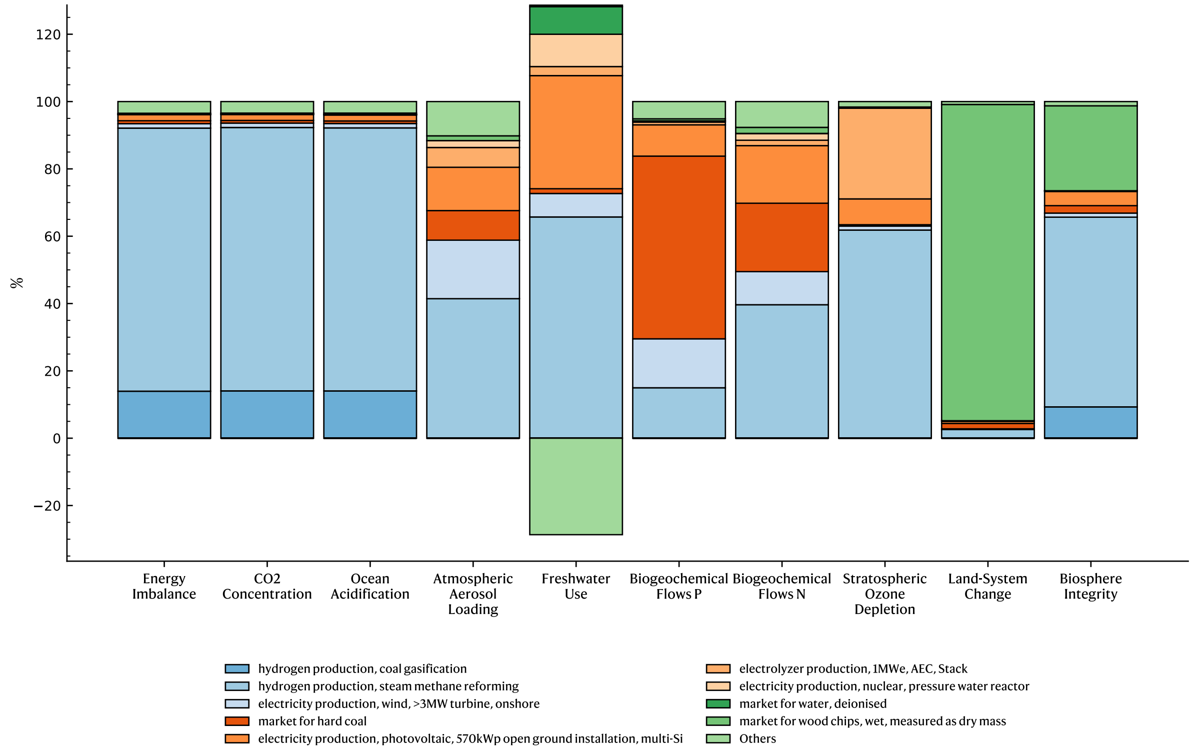

Figure 15. **Contribution analysis for 2025 and SSP2 scenario.**

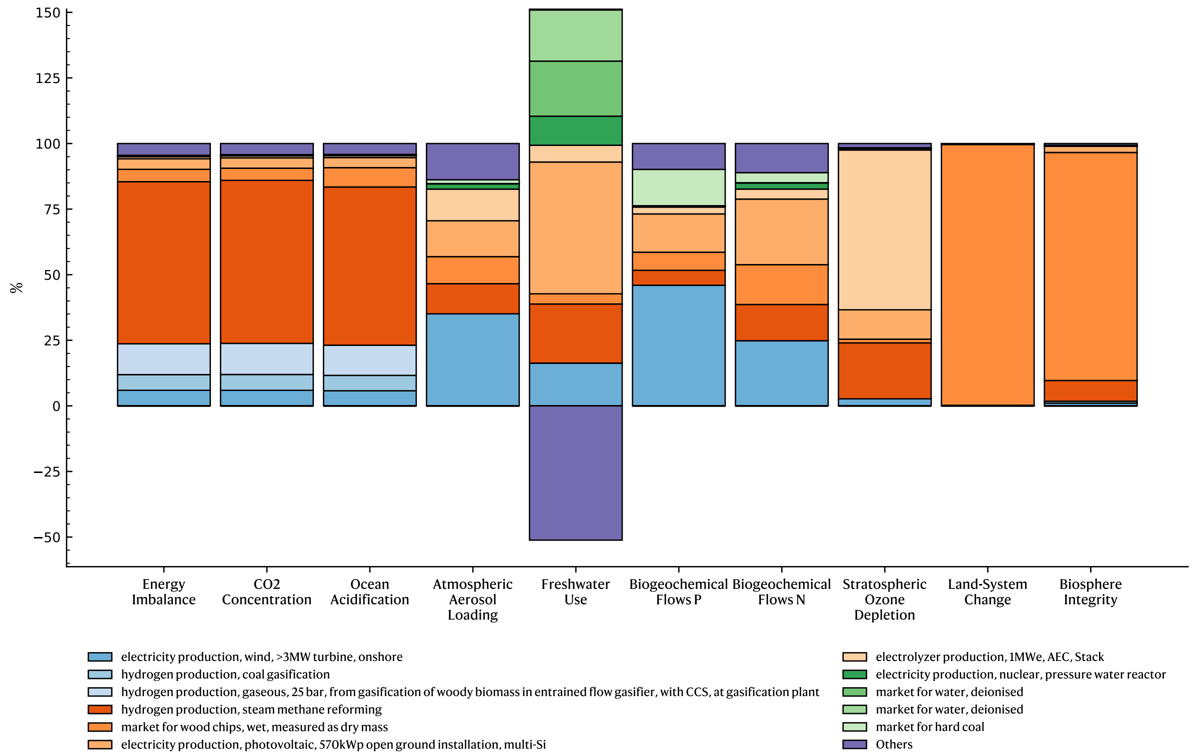

Figure 16. **Contribution analysis for 2030 and SSP2 scenario.**

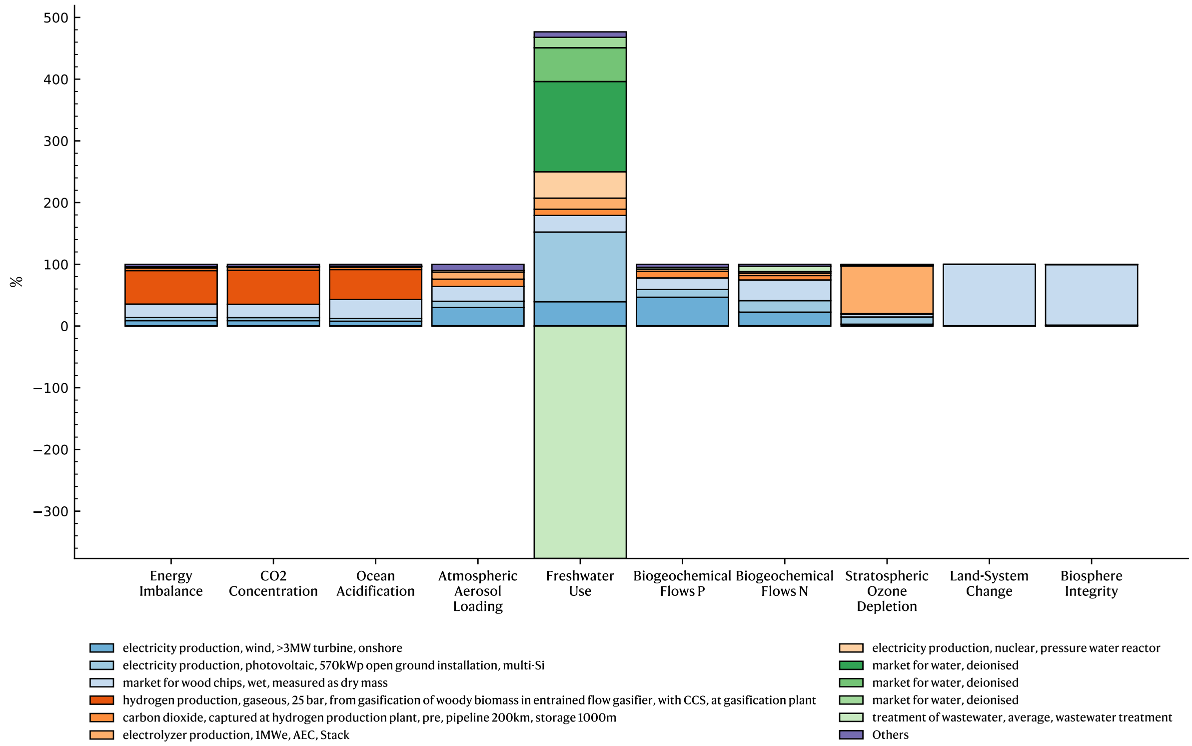

Figure 17. **Contribution analysis for 2040 and SSP2 scenario.**

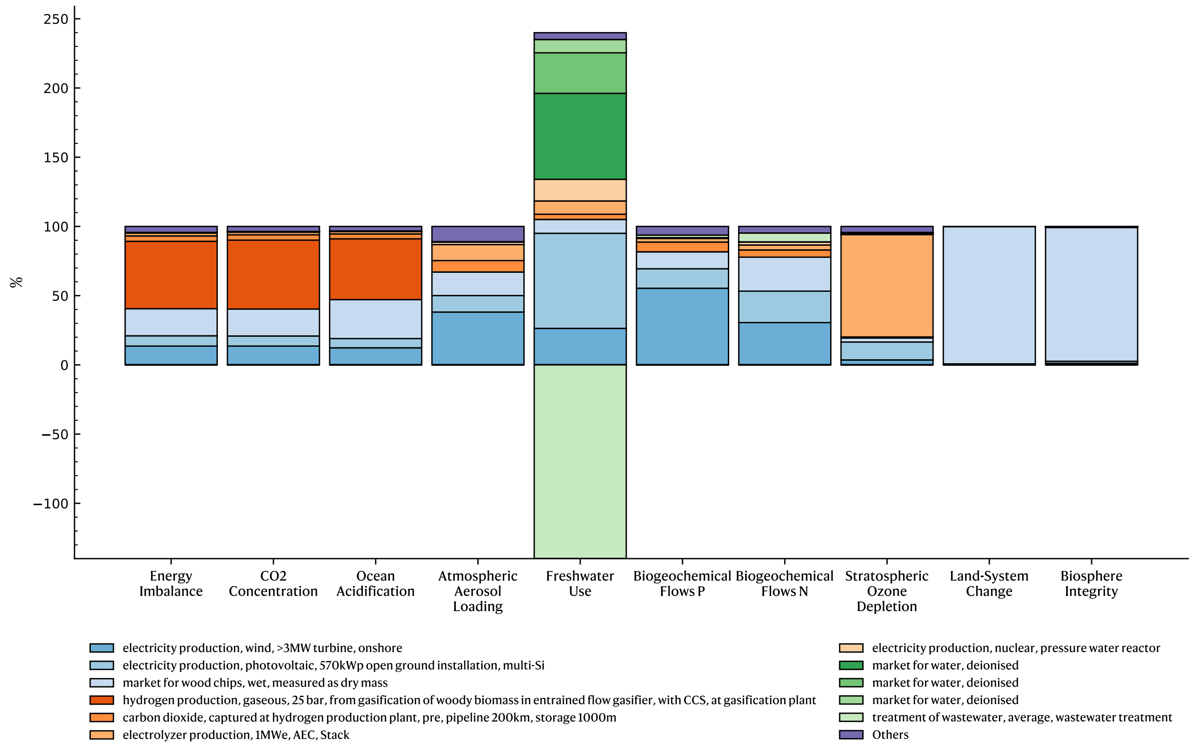

Figure 18. **Contribution analysis for 2050 and SSP2 scenario.**

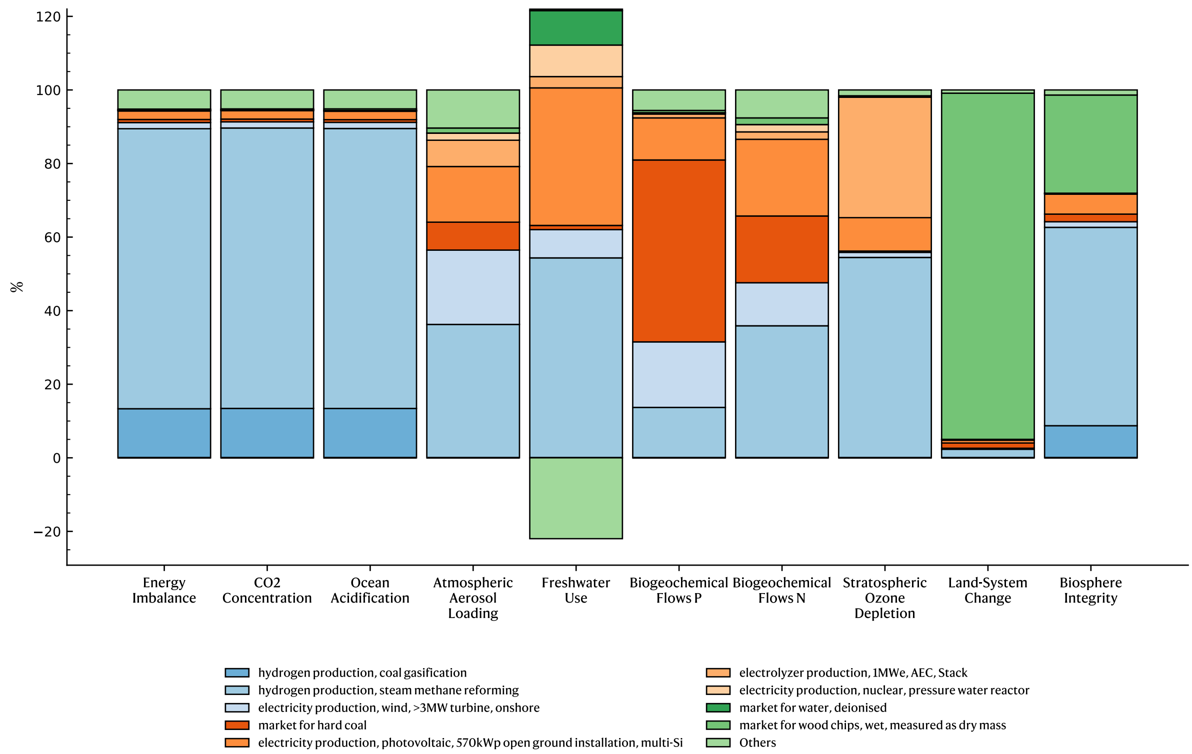

Figure 19. **Contribution analysis for 2025 and SSP5 scenario.**

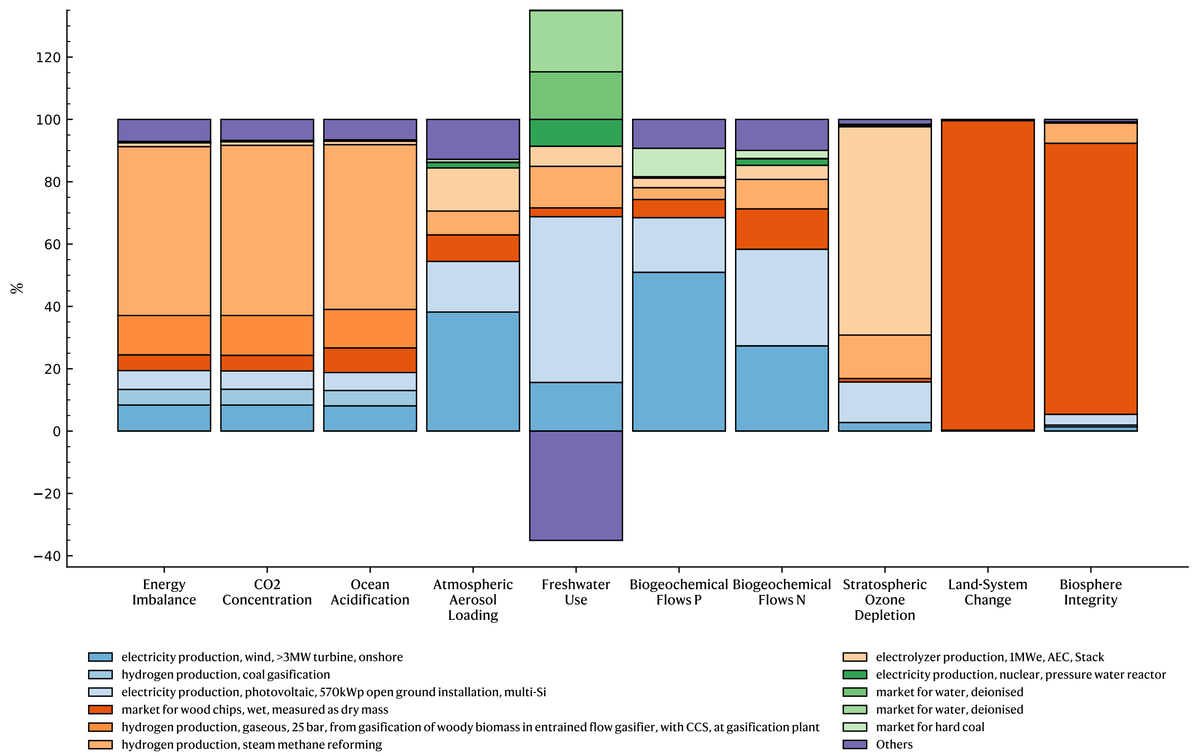

Figure 20. **Contribution analysis for 2030 and SSP5 scenario.**

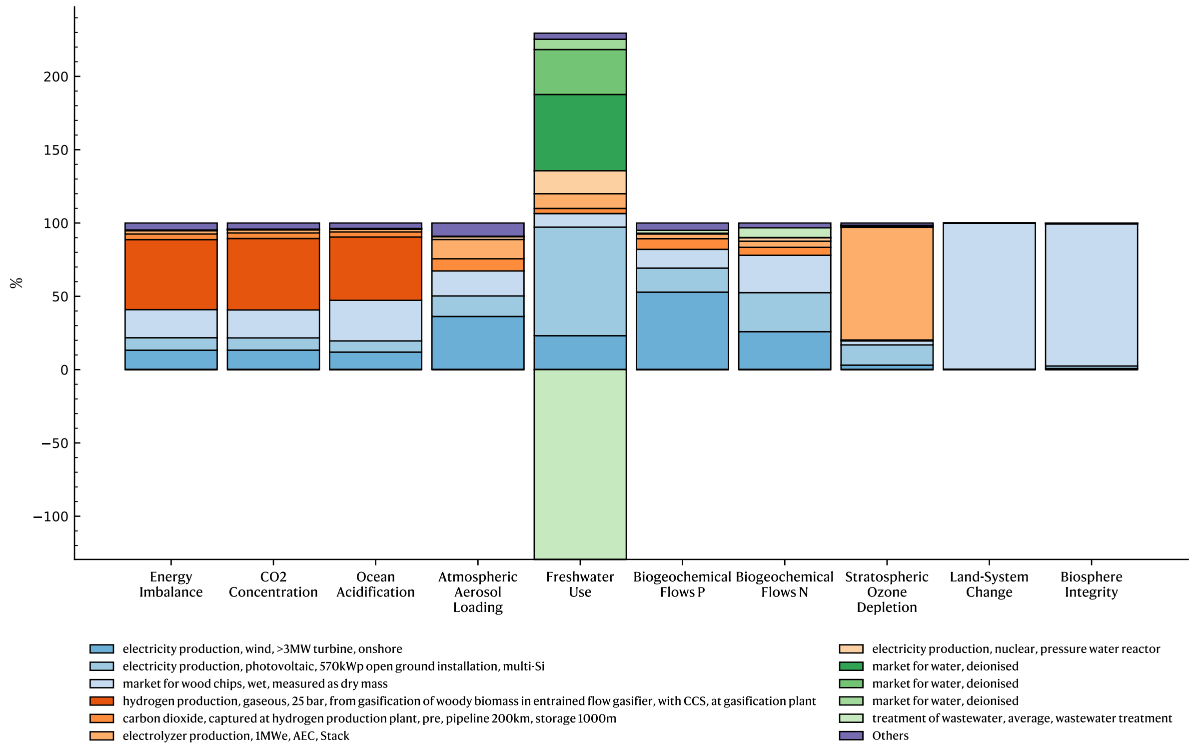

Figure 21. **Contribution analysis for 2040 and SSP5 scenario.**

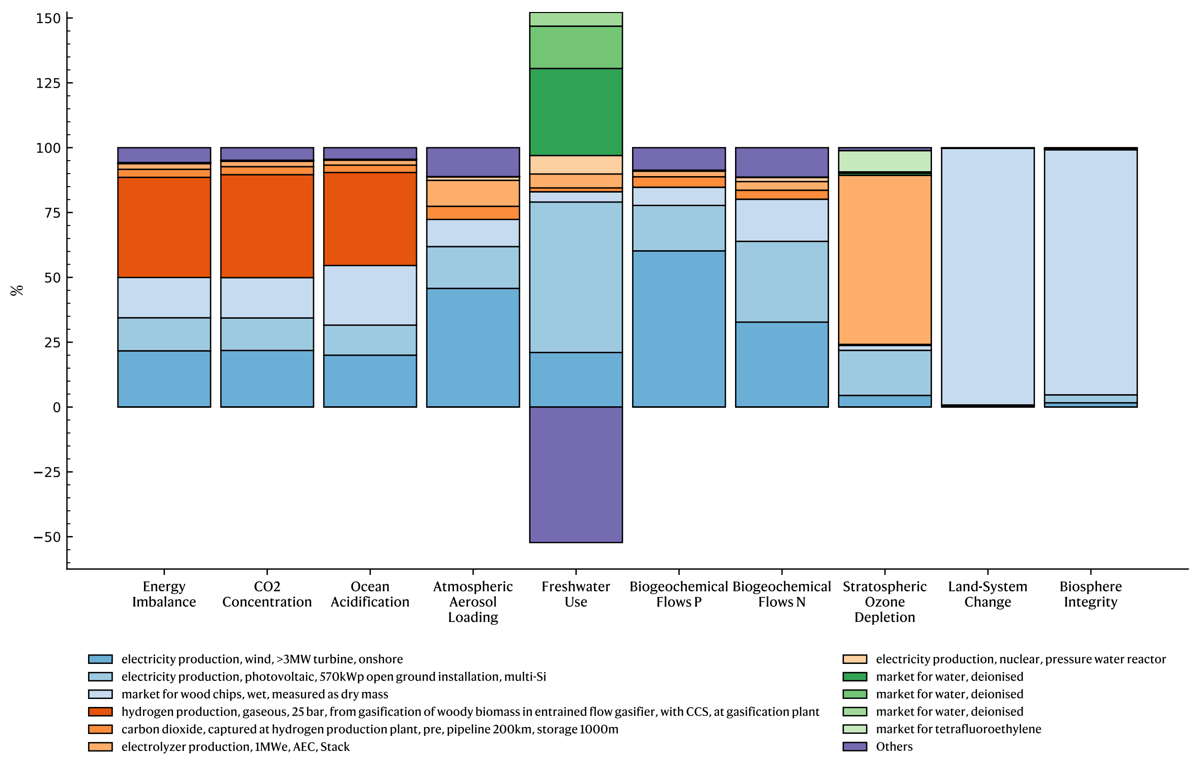

Figure 22. **Contribution analysis for 2050 and SSP5 scenario.**

Sensitivity between scenarios

This section details the relative difference between SSP and planetary boundary interaction scenarios. The main script focuses on the SSP1-PkBudg500 and the B-PBI scenarios for the impact assessment. This section aims to contrast more with the SSP2, SSP5-PkBudg500 scenarios and the H-PBI scenarios.

Figure 23 shows the relative difference of the absolute sustainability ratio in the SSP2 and SSP5 scenarios with the SSP1-PkBudg500 and in each planetary boundary interaction scenario. In addition to that, Figure 24 shows the relative difference between the H-PBI and B-PBI scenarios.

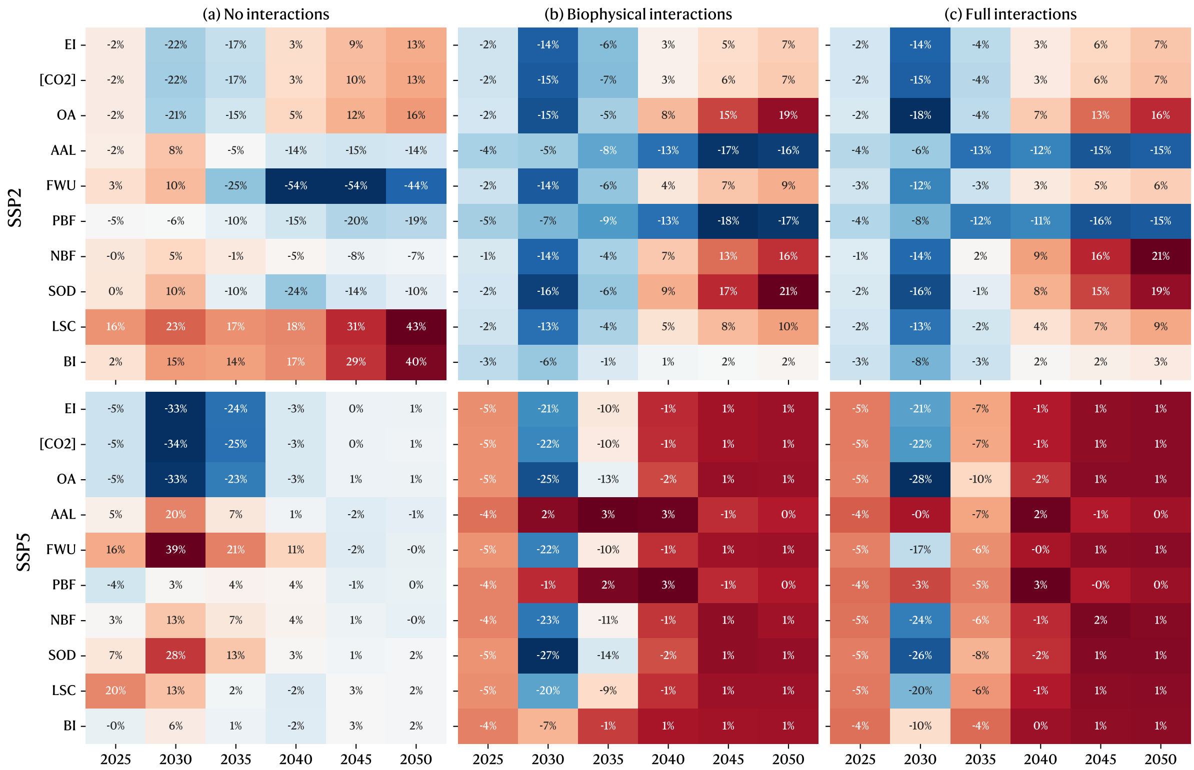

Figure 23. **Difference in planetary footprint for the SSP2 and SSP5 scenarios relative to SSP1**. EI = Energy imbalance (change in radiative forcing). $[CO_2]$ = Change CO_2 concentration. OA= Ocean acidification. AAL = Atmospheric aerosol loading. FWU = Freshwater use. PBF = phosphorus biochemical flow. NBF = Nitrogen biochemical flow. SOD = Stratospheric ozone depletion. LSC = Land system change. BI = Biosphere integrity.

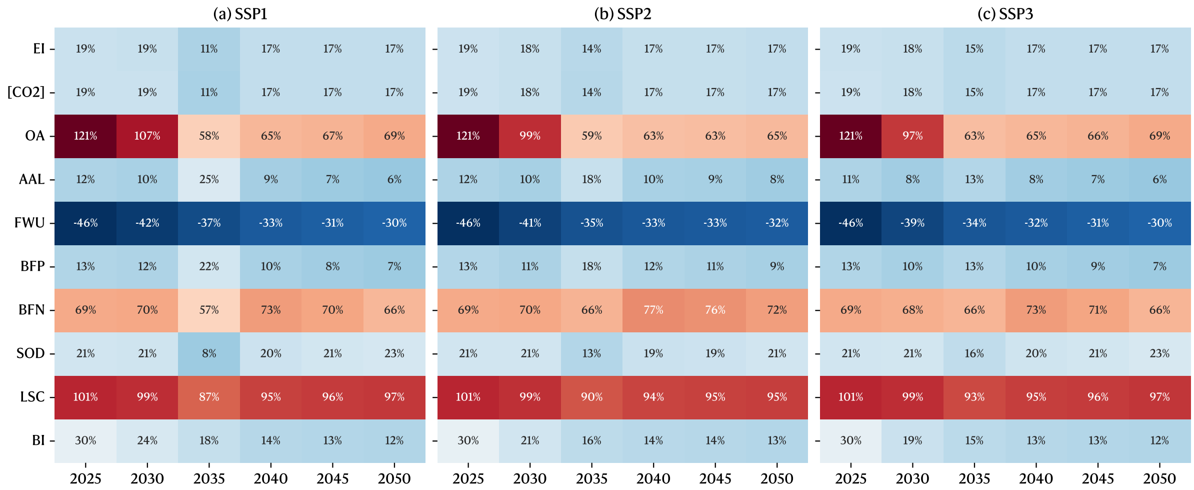

Figure 24. **Planetary footprint difference of the H-PBI scenario relative to B-PBI for each SSP scenario.** EI = Energy imbalance (change in radiative forcing). [CO_2] = Change CO_2 concentration. OA= Ocean acidification. AAL = Atmospheric aerosol loading. FWU = Freshwater use. PBF = phosphorus biochemical flow. NBF = Nitrogen biochemical flow. SOD = Stratospheric ozone depletion. LSC = Land system change. BI = Biosphere integrity.

Extended sensitivity analysis

This section extends the sensitivity analysis relating to the effect of global hydrogen production with (i) concurrent carbon removal only and (ii) increased electrolysis capacity with concurrent carbon capture. The main script mainly focuses on the B-PBI scenario. Thus, this section performs the same sensitivity analysis for the H-PBI scenario. Subsequently, we study the effect of opting for an unconstrained nuclear energy supply for the increased electrolytic hydrogen capacity.

Effect of carbon removal in the H-PBI scenario

When focusing on the full range of interactions as opposed to the interpretation from the main script, we find that a lower capture rate would be required to be sustainable in the biosphere integrity boundary (see Figure 25). The difference can be attributed to the stronger interaction parameters (Figure 6). Thus, capturing atmospheric carbon dioxide has a stronger effect on all boundaries. Yet, despite these stronger interactions, these results show that the interpretation made in the main script remains valid. Under this scenario, global hydrogen production would remain unsustainable in the PBF and AAL boundaries and reaching the aSOS boundary in the BI boundary would imply trade-offs with that of the FWU, SOD boundaries.

Similarly, increasing the electrolytic hydrogen production capacity in the H-PBI scenario (Figure 26) leads to conclusions similar to those in the main script. Again, the difference in the result lies in the stronger interaction parameters for the H-PBI scenario.

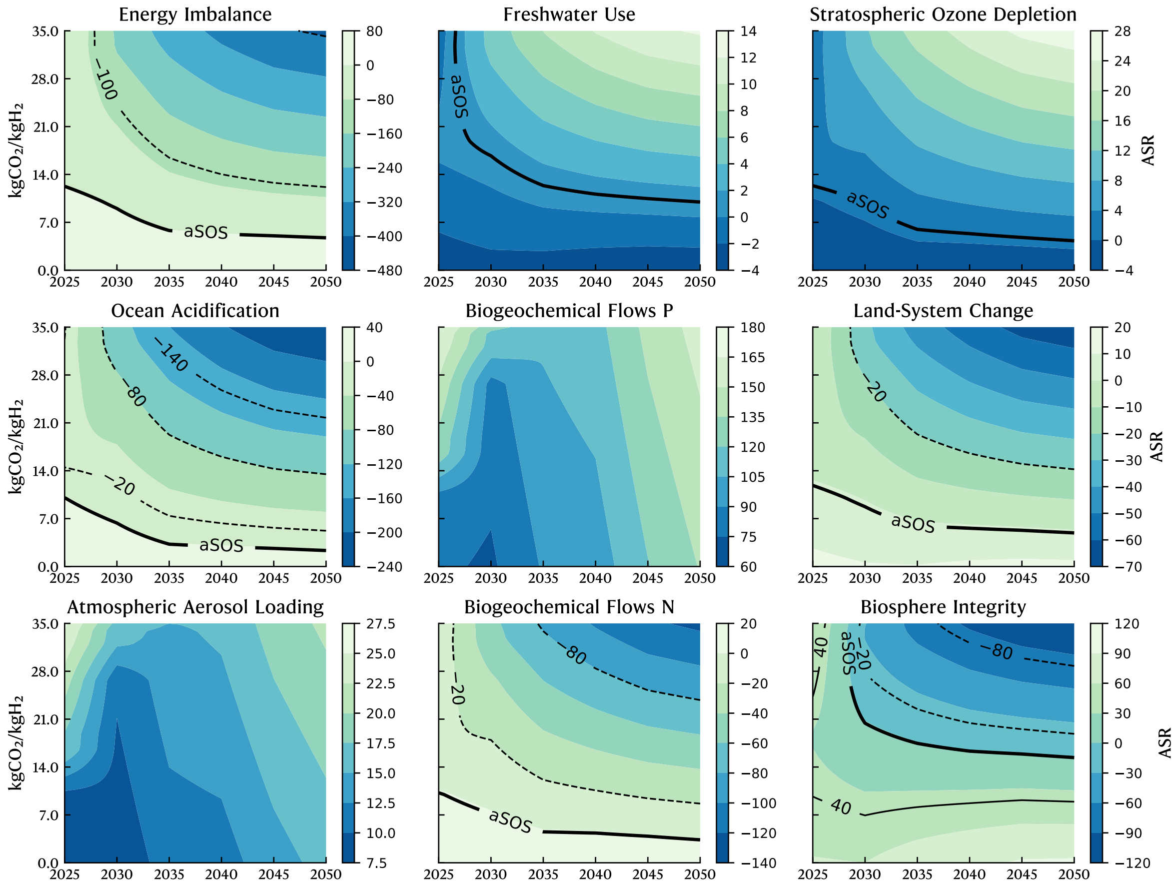

Figure 25. **Effect of carbon removal in the SSP1 and H-PBI scenario.** Dark blue shows the lowest, and light green has the strongest impact. The bold and solid aSOS line shows its boundary.

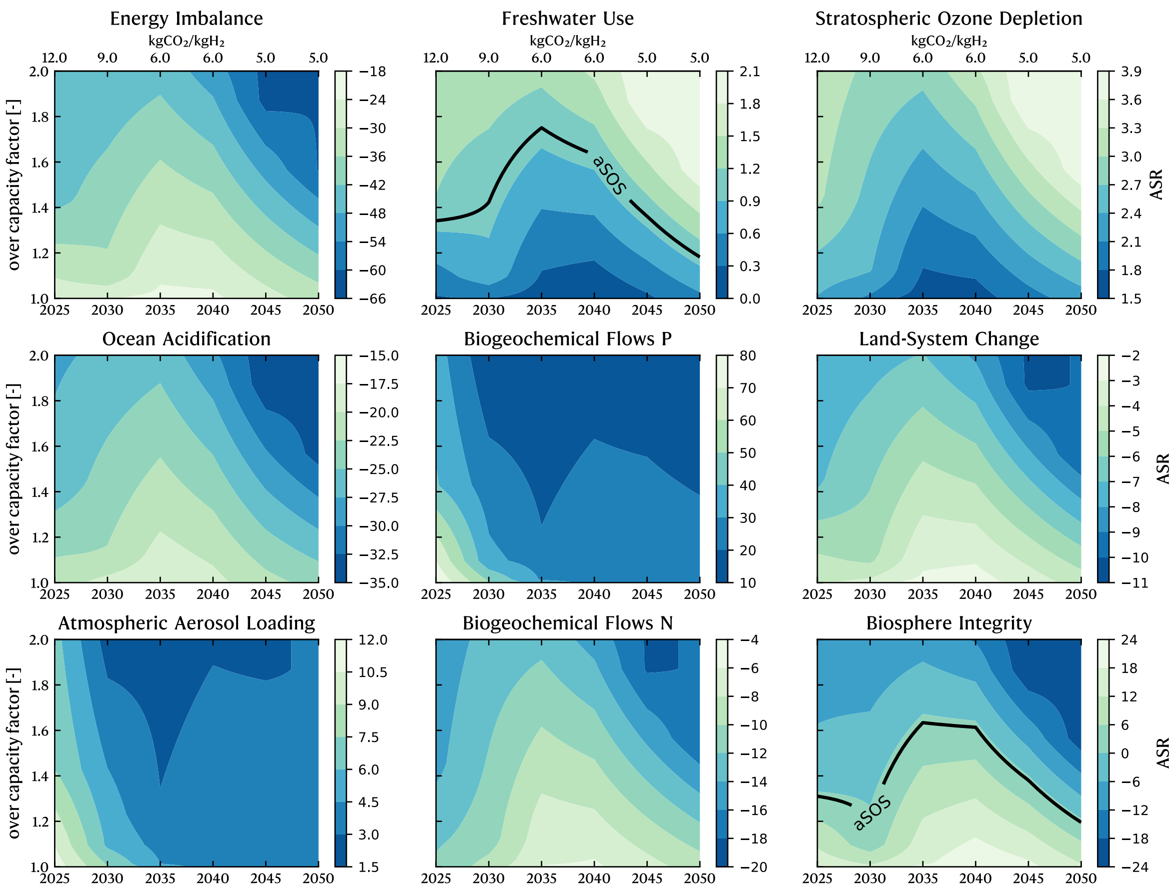

Figure 26. **Effect of an increased electrolysis capacity with concurrent carbon capture in the SSP1 and H-PBI scenario**. The dark blue area shows the lowest impact, while the light green shows the strongest.

Effect of an unconstrained nuclear energy supply

In the main script, a sensitivity analysis of the increase in electrolytic hydrogen production capacity is performed. To this extent, the hydroelectricity supply is purposefully unconstrained as this source shows the lowest impact on the boundary for climate change (see Figure 27). As can be seen from Figure 27, for the BI boundary, nuclear energy shows the lowest impact. Because the BI boundary is as important as the climate change boundary, we found necessary to show sensitivity results with an unconstrained nuclear energy supply. Results for these sensitivity analyses are represented in Figure 28 for the B-PBI scenario and Figure 29 for the H-PBI scenario.

Although nuclear energy shows the best environmental performance in the BI boundary, compared to Figure 5 of the main script, the aSOS of the BI boundary is found to be more difficult to achieve. Indeed, focusing on the minimum ASR values for nuclear energy would lead to a stronger impact on the CC, AAL, and PBF boundaries. Given the interaction parameters in the B-PBI scenario, the minimum achievable in the BI boundary would be less feasible. Similar conclusions can also be drawn in the H-PBI scenario. Given that, conclusions reported in the main script would remain valid in this sensitivity analysis.

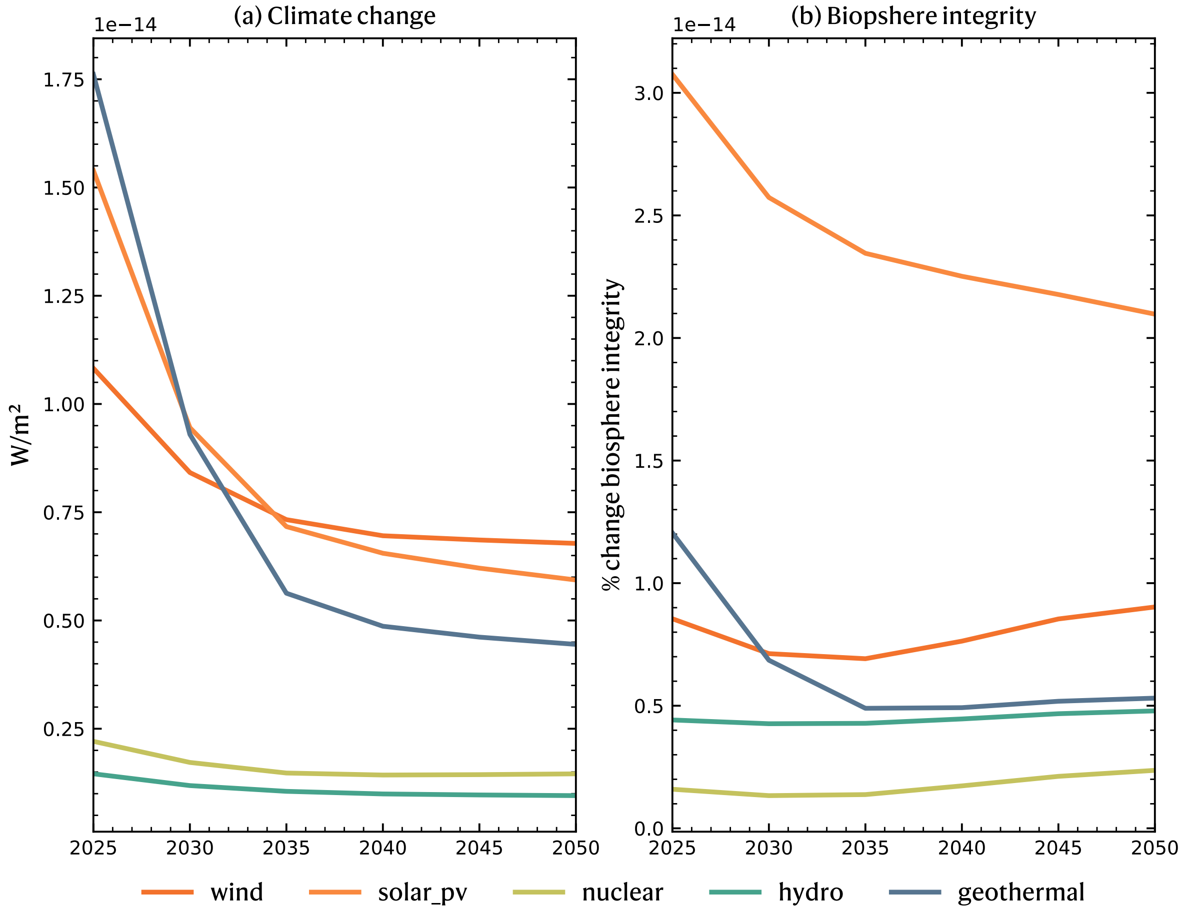

Figure 27. **Absolute impact on the radiative forcing and biosphere integrity boundary per energy source.** Comparison of low emissions electricity sources. pv = photovoltaic.

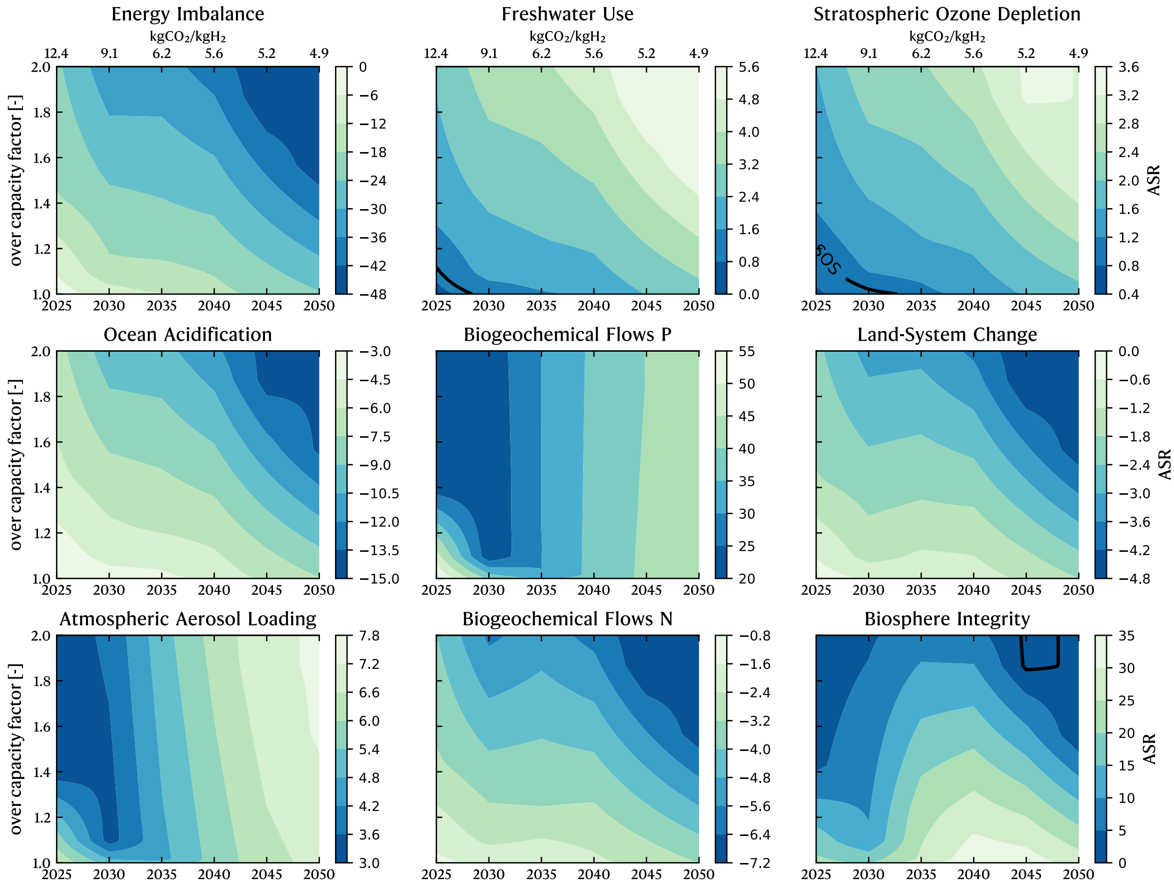

Figure 28. **Effect of an increased electrolysis capacity with concurrent carbon capture in the SSP1 and B-PBI scenario with unconstrained nuclear energy**. The dark blue area shows the lowest impact, while the light green shows the strongest.

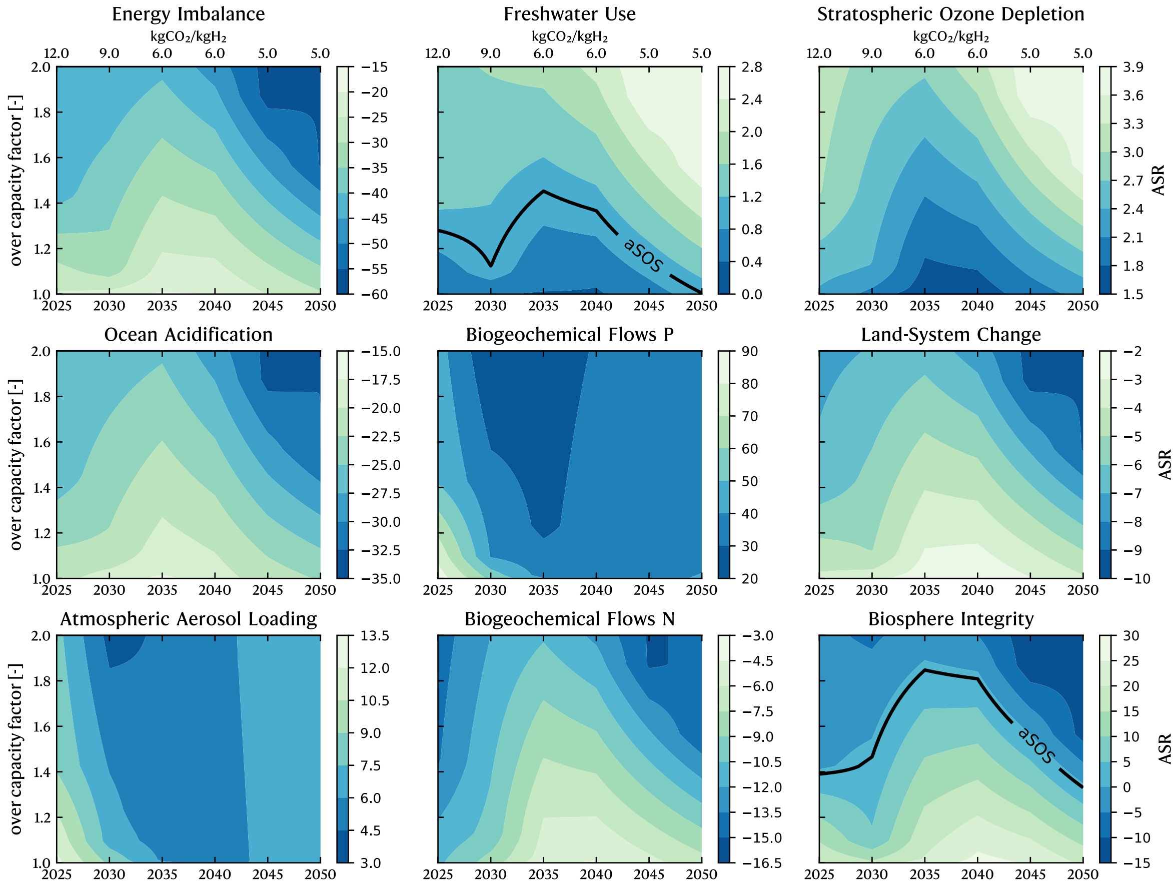

Figure 29. **Effect of an increased electrolysis capacity with concurrent carbon capture in the SSP1 and H-PBI scenario with unconstrained nuclear energy**. The dark blue area shows the lowest impact, while the light green shows the strongest.

References

1. Byers, E. *et al.* AR6 Scenarios Database. Integrated Assessment Modeling Consortium & International Institute for Applied Systems Analysis https://doi.org/10.5281/ZENODO.5886911 (2022).
2. *Climate Change 2022: Mitigation of Climate Change*. (IPCC, Geneva, 2022).
3. Bjørn, A. *et al.* Review of life-cycle based methods for absolute environmental sustainability assessment and their applications. *Environ. Res. Lett.* **15**, 083001 (2020).
4. Heide, M., Hauschild, M. Z. & Ryberg, M. Reflecting the importance of human needs fulfilment in absolute sustainability assessments: Development of a sharing principle. *J. Ind. Ecol.* **27**, 1151–1164 (2023).
5. Hjalsted, A. W. *et al.* Sharing the safe operating space: Exploring ethical allocation principles to operationalize the planetary boundaries and assess absolute sustainability at individual and industrial sector levels. *J. Ind. Ecol.* **25**, 6–19 (2021).
6. Heide, M. & Gjerris, M. Embedded but overlooked values: Ethical aspects of absolute environmental sustainability assessments. *J. Ind. Ecol.* **28**, 386–396 (2024).
7. Heide, M., Dudka, K. M. & Hauschild, M. Z. Absolute sustainable CO2-limits for buildings should reflect their function. A case study of four building typologies. *Dev. Built Environ.* **15**, 100175 (2023).
8. Weidner, T., Tulus, V. & Guillén-Gosálbez, G. Environmental sustainability assessment of large-scale hydrogen production using prospective life cycle analysis. *Int. J. Hydrog. Energy* S0360319922052570 (2022) doi:10.1016/j.ijhydene.2022.11.044.
9. Salah, C., Cobo, S., Pérez-Ramírez, J. & Guillén-Gosálbez, G. Environmental Sustainability Assessment of Hydrogen from Waste Polymers. *ACS Sustain. Chem. Eng.* **11**, 3238–3247 (2023).
10. D'Angelo, S. C. *et al.* Planetary Boundaries Analysis of Low-Carbon Ammonia Production Routes. *ACS Sustain. Chem. Eng.* **9**, 9740–9749 (2021).
11. D'Angelo, S. C., Mache, J. & Guillén-Gosálbez, G. Absolute Sustainability Assessment of Flue Gas Valorization to Ammonia and Synthetic Natural Gas. *ACS Sustain. Chem. Eng.* **11**, 17718–17727 (2023).
12. Guinée, J. B., de Koning, A. & Heijungs, R. Life cycle assessment-based Absolute Environmental Sustainability Assessment is also relative. *J. Ind. Ecol.* (2022) doi:10.1111/jiec.13260.
13. Meinshausen, M. *et al.* The SSP greenhouse gas concentrations and their extensions to 2500. Preprint at https://doi.org/10.5194/gmd-2019-222 (2019).
14. Baumstark, L. *et al.* REMIND2.1: transformation and innovation dynamics of the energy-economic system within climate and sustainability limits. *Geosci. Model Dev.* **14**, 6571–6603 (2021).

15. Sacchi, R. *et al.* PRospective EnvironMental Impact asSEment (premise): A streamlined approach to producing databases for prospective life cycle assessment using integrated assessment models. *Renew. Sustain. Energy Rev.* **160**, 112311 (2022).

16. Calvin, K. *et al. IPCC, 2023: Climate Change 2023: Synthesis Report. Contribution of Working Groups I, II and III to the Sixth Assessment Report of the Intergovernmental Panel on Climate Change [Core Writing Team, H. Lee and J. Romero (Eds.)]. IPCC, Geneva, Switzerland.* https://www.ipcc.ch/report/ar6/syr/ (2023) doi:10.59327/IPCC/AR6-9789291691647.

17. IEA. *Net Zero by 2050 - A Roadmap for the Global Energy Sector*. 224 https://www.iea.org/reports/net-zero-by-2050 (2021).

18. Alšauskas, O. World Energy Outlook 2024.

19. Charalambous, M. A., Sacchi, R., Tulus, V. & Guillén-Gosálbez, G. Integrating emerging technologies deployed at scale within prospective life cycle assessments. *Sustain. Prod. Consum.* **50**, 499–510 (2024).

20. Lechtenberg, F. *et al.* PULPO: A framework for efficient integration of life cycle inventory models into life cycle product optimization. *J. Ind. Ecol.* **n/a**, (2024).

21. Ryberg, M. W., Bjerre, T. K., Nielsen, P. H. & Hauschild, M. Absolute environmental sustainability assessment of a Danish utility company relative to the Planetary Boundaries. *J. Ind. Ecol.* **25**, 765–777 (2021).

22. Richardson, K. *et al.* Earth beyond six of nine planetary boundaries. *Sci. Adv.* **9**, eadh2458 (2023).

23. Wei, S., Sacchi, R., Tukker, A., Suh, S. & Steubing, B. Future environmental impacts of global hydrogen production. *Energy Environ. Sci.* (2024) doi:10.1039/D3EE03875K.

24. Terlouw, T., Rosa, L., Bauer, C. & McKenna, R. Future hydrogen economies imply environmental trade-offs and a supply-demand mismatch. *Nat. Commun.* **15**, 7043 (2024).

25. Gerloff, N. Comparative Life-Cycle-Assessment analysis of three major water electrolysis technologies while applying various energy scenarios for a greener hydrogen production. *J. Energy Storage* **43**, 102759 (2021).

26. Antonini, C. *et al.* Hydrogen production from natural gas and biomethane with carbon capture and storage – A techno-environmental analysis. *Sustain. Energy Fuels* **4**, 2967–2986 (2020).

27. *Transition to Hydrogen: Pathways toward Clean Transportation*. (Cambridge University Press, Cambridge, 2011). doi:10.1017/CBO9781139018036.

28. Al-Qahtani, A., Parkinson, B., Hellgardt, K., Shah, N. & Guillen-Gosalbez, G. Uncovering the true cost of hydrogen production routes using life cycle monetisation. *Appl. Energy* **281**, 115958 (2021).

29. Zhang, J., Ling, B., He, Y., Zhu, Y. & Wang, Z. Life cycle assessment of three types of hydrogen production methods using solar energy. *Int. J. Hydrog. Energy* **47**, 14158–14168 (2022).

30. Wernet, G. *et al.* The ecoinvent database version 3 (part I): overview and methodology. *Int. J. Life Cycle Assess.* **21**, 1218–1230 (2016).

31. Volkart, K., Bauer, C. & Boulet, C. Life cycle assessment of carbon capture and storage in power generation and industry in Europe. *Int. J. Greenh. Gas Control* **16**, 91–106 (2013).

32. Qiu, Y. *et al.* Environmental trade-offs of direct air capture technologies in climate change mitigation toward 2100. *Nat. Commun.* **13**, 3635 (2022).

33. Lade, S. J. *et al.* Human impacts on planetary boundaries amplified by Earth system interactions. **3**, 119–128 (2020).

34. Kätelhön, A., Bardow, A. & Suh, S. Stochastic Technology Choice Model for Consequential Life Cycle Assessment. *Environ. Sci. Technol.* **50**, 12575–12583 (2016).